Charles University In Prague

Faculty of Science
Department of Biochemistry

Bc. Ivica Krištofičová

Study of the cleavage kinetics of Gag polyprotein from HIV-1 virus by the viral proteinase

Studium kinetiky štěpení polyproteinu Gag z viru HIV-1 virovou proteinasou

Diploma Thesis

Supervisor : RNDr. Marek Ingr, Ph.D.
Consultants : Doc. RNDr. Jan Konvalinka, CSc.
Mgr. Klára Grantz Šašková, Ph.D.

Prague 2013

Prohlášení

Prohlašuji, že jsem tuto diplomovou práci vypracovala samostatně pod vedením školitele Marka Ingra a všechny použité prameny jsem řádně citovala.

Místo a datum : Podpis :

Acknowledgements

Looking back two years since I came to Prague, it was an amazing experience! I would like to thank all people who support my research and made this thesis possible.

At first, I would like to thank Honza Konvalinka that he gave me a place to sit and pipet. He introduced me to wonders and frustrations of science and his devoted attitude in research inspired me a lot.

Special thanks to Klára Grantz-Šašková who taught me all the laboratory skills and brought me this far. She has made me engaged and entertained at the same time.

My gratitude also goes to my supervisor Marek Ingr who has encouraged me and always believed in successfully completed experiments.

The best motivation in my work are my colleagues at IOCB. They create very challenging and friendly atmosphere. My huge thanks to Milan Kožíšek, Monika Sivá, Michal Svoboda, Iva Flaisigová and many others.

Last but no least, I feel indebted to my parents for their support and love during my studies and to my brother Milutin who was always near when I needed him. And of course, I thank my friend Stanislav for his moral encouragement and listening to my good and bad lab days even he does not understand a word.

Abstract

Gag polyprotein is the precursor of HIV-1 structural proteins, required for correct assembly, budding and maturation of viral particle within HIV-1 life cycle. The process of maturation into an infectious virion is dependent on Gag and GagPol cleavage at nine predefined sites by HIV-1 proteinase. Its disruption is one of the main targets of HIV treatment. HIV-1, however, develops resistance to the proteinase inhibitors by creating mutations in both the proteinase and the substrate.

The Gag processing by HIV-1 proteinase is a highly sequential process, that happens in specific order and rate. Previous biochemical studies determined the kinetic data of these processes using oligopeptides representing naturally occuring cleavage sites. This thesis describes the cleavage of the Gag polyprotein itself, which is the natural substrate of HIV-1 proteinase. For this purpose, the full-length Gag polyprotein was recombinantly prepared in bacterial expression system. The cleavage was carried out and its products were analyzed via SDS-PAGE and Western blotting. The substrate specificity of the wild-type and mutant HIV-1 proteinase with respect to the full-length wild-type Gag polyprotein was compared. Substantial differences were observed between the rates of individual steps of cleavage by the wild-type and mutant HIV-1 proteinase.

Key words: HIV, Gag, kinetics, proteinase, inhibitor, drug resistance

Abstrakt

Polyprotein Gag je prekurzorem strukturních proteinů viru HIV-1 nezbytných pro správné složení, pučení a zrání virové částice v průběhu životního cyklu viru HIV-1. Proces zrání do stádia infekčního virionu je závislý na štěpení polyproteinu Gag a GagPol virovou proteinasou na devíti přesně určených místech. Narušení tohoto štěpení je jedním z hlavních terapeutických cílů v léčbě nákazy HIV. Virus HIV-1 si však vytváří rezistenci k inhibitorům proteinasy vznikem mutací jak v proteinase samotné, tak v jejím substrátu.

Štěpení Gagu HIV-1 proteinasou je proces s přesně daným pořadím a rychlostí jednotlivých kroků. Předchozí biochemické studie stanovily kinetické parametry těchto procesů s pomocí oligopeptidů reprezentujících přirozeně se vyskytující štěpicí místa. Tato práce popisuje štěpení samotného polyproteinu Gag, který je přirozeným substrátem HIV-1 proteinasy. Za tímto účelem byl rekombinantně připraven kompletní polyprotein Gag v bakteriálním expresním systému. Bylo provedeno jeho štěpení HIV-1 proteinasou a produkty tohoto štěpení byly analyzovány pomocí SDS-PAGE a Western blotu. Dále byla porovnána substrátová specifita proteinasy divokého typu a mutované varianty HIV-1 proteinasy vůči kompletnímu divokému typu Gag polyproteinu. Byly pozorovány podstatné rozdíly mezi rychlostmi jednotlivých kroků štěpení pomocí proteinasy divokého typu a mutované HIV-1 proteinasy.

Kľúčové slová: HIV, Gag, kinetika, proteinasa, inhibitor, rezistence vůči léčivu

Contents

List of Abbreviations

AIDS	Acquired Immunodeficiency Syndrome
AMP	Ampicillin
APS	Ammonium Persulfate
BSA	Bovine Serum Albumin
CA	Capsid
CDC	Centers for Disease Control and Prevention
CTD	C-terminal Domain
DMSO	Dimethyl Sulfoxide
EDTA	Ethylenediaminetetraacetic Acid
FDA	Food and Drug Administration
HAART	Highly Active Anti-Retroviral Therapy
HIV	Human Immunodeficiency Virus
IN	Integrase
IPTG	Isopropyl-β-D-thiogalaktopyranosid
MA	Matrix
NC	Nucleocapsid

NTD	N-terminal Domain
PI	Proteinase Inhibitor
PIC	Preintegration Complex
PR	Proteinase
RT	Reverse Transcriptase
RTC	Reverse Transcription Complex
SDS	Sodium Dodecyl Sulfate
SIV	Simian Immunodeficiency Virus
SU	Surface protein
TEMED	Tetramethylethylenediamine
TFP	Transframe protein
TM	Transmembrane protein
TRIS	Tris(hydroxymethyl)aminoethan
WHO	World Health Organization

Chapter 1

Introduction

Acquired Immunodeficiency Syndrome (AIDS) was described by Centers for Disease Control and Prevention (CDC) in July 1982. Soon, its causative agent was identified by team of French scientists led by Luc Montagnier [1] and American scientists led by Robert Charles Gallo [2]. The virus was named the Human Immunodeficiency Virus (HIV) by the International Committee on Taxonomy of Viruses. There are two strains of HIV: HIV-1 and HIV-2 [3]. They share 50% homology and differ in pathogenicity (the ratio of infectivity HIV-1/HIV-2 is 3.6) and geographic location [4, 5].

HIV is a member of the Retroviridae family, genus lentivirus. The infection is usually transmitted via sexual intercourse. The transmission via blood transfusion or from pregnant mother to her child was significantly decreased due to blood control and antiviral therapy, respectively. HIV attacks human immune system and reduces the number of its vital cells, in particular dendritic cells, macrophages and mainly CD4+ Th cells [6]. Thus organism is unable to protect itself from various opportunistic infections and people die due to immune system failure.

AIDS is still one of the most numbered lethal disease in the world. According to World Health Organization (WHO), around 34 million people live with HIV and there are 1.7 million deaths due to AIDS according to statistics of the HIV infection in 2011 [7]. Unfortunately and despite all the prevention work, the number of patients is still increasing mainly in regions of subsaharian Africa.

The aim of the anti-HIV therapy is to significantly decrease the viral load and to enhance patient's immunity by increasing CD4+ cells. Patients are usually treated with a highly active antiviral therapy (HAART), treatment that combines drugs of different targets of the viral life cycle and inhibit HIV replication. This results in prolonged life expectancy and decreased mortality of the patients.

Unfortunately, the virus is highly variable, and the mutations cause resistance to all approved medicaments. Therefore new active compounds with different mode of action, simple dosage and lower toxicity are still needed. To achieve that goal we have to understand all the steps the virus takes during its life cycle in order to reproduce.

1.1 HIV-1 Life Cycle

The HIV-1 replication cycle (**Figure 1.1**) is a multistep process regulated by viral and cellular proteins, that lasts for 1.2 days and generates up to 10^{10} virions daily [8]. The process starts when viral surface glycoprotein gp120 binds to chemokine receptors of the human CD4+ cells and interacts with its coreceptors, CXCR4 and CCR5 [9]. This induces conformational changes in gp120 subunit and transmembrane protein gp41 [10], which result in a membrane fusion reaction. The viral core, that consists of capsid (CA) and nucleocapsid proteins (NC), genomic RNA and three viral enzymes: HIV-1 proteinase (PR), integrase (IN) and reverse transcriptase (RT), is released into the cell cytoplasm [11].

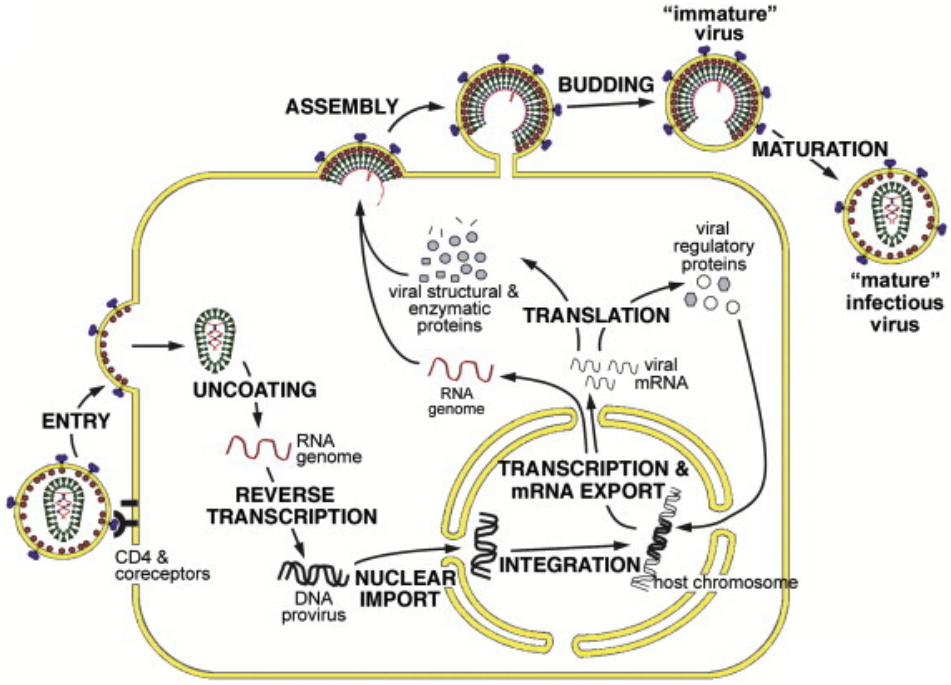

Figure 1.1: The replication cycle of HIV-1. Adopted from [12].

After the fusion, RNA is uncoated in several steps that are not complementely understood. Some of the structural proteins (matrix - MA and NC), enzymes (IN, RT) and accessory protein Vpr are associated with a reverse transcription complex (RTC), that generates the double stranded DNA from viral ssRNA. CA is completely degraded [13]. Later on, the preintegration complex (PIC) harbouring viral DNA is formed. PIC inter-

acts with nucleoporins in the nuclear envelope and is transported into the host nucleus by yet unknown mechanism [14]. The viral integrase incorporates viral DNA into the host chromosome. The integrated viral DNA is called the provirus [11] and serves as a template to create new viral RNAs that encode nine genes for successful virus replication (*gag, pol, env, nef, rev, tat, vif, vpr* and *vpu*).

The assembly process takes place at the plasma membrane of the cell. The Gag polyprotein binds to the membrane by myristic acid moiety and recruits two copies of ssRNA. The assembled Gag polyprotein mediates Gag-Gag interactions and the formation of budding particle. The Gag specific sequence refered to as "L" or "late" domain located in p6 in Gag promotes the release of the immature virion from the cell. The mechanisms of the release stimulation is not yet elucidated [15, 16]. Immediately after or during budding, the viral PR cleaves Gag and GagPol polyproteins. It leads to viral maturation, during which the rearrangement of the particle and core condensation occurs. Thus the virion becomes infectious.

1.2 HIV-1 Genome and Protein Architecture

HIV virion contains diploid genome (**Figure 1.2** on page 14) - 2 molecules of ssRNA (9 kb), replicated by reverse transcriptase (RT). RNA encodes 9 genes, that are overlapping and which are synthesized in a form of three main polypeptides : Gag, GagPol and Env. They have to be proteolytically cleaved by viral or bacterial proteinase to become functional. The Gag polypeptide is cleaved to structural proteins of the virion, *pol* codes viral enzymes and *env* codes glycoproteins of the virion envelope that help to infect the target cell.

Translation of the *gagpol* gene leads to the proteosynthesis of either Gag (p55) or GagPol (p160) polyproteins. In majority of cases the translation is terminated by the stop-codon located in the p6 region of the gene which results in Gag production. However, in 5-10 % cases, a -1 ribosomal frameshift occurs that changes the open reading frame and GagPol is synthesized [17]. The polyproteins are furthermore cotranslationally myristoylated [18].

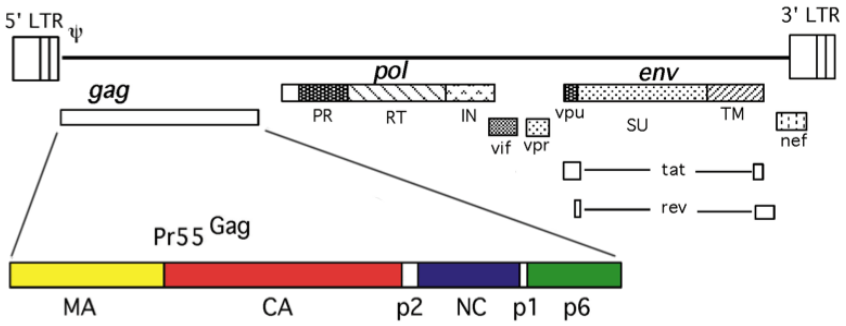

Figure 1.2: The HIV-1 genome. ssRNA codes polyproteins Gag, Pol, Env. The *gag* gene codes structural proteins (MA,CA, NC and p6), *env* gene codes envelope glycoproteins (SU and TM) and *pol* gene encodes viral enzymes PR, RT and IN. Adopted from [11].

Gag polyprotein

Gag polyprotein is a precursor of several structural proteins of HIV similarly to other retroviruses such as Rous sarcoma virus, Moloney murine leukemia virus and Mason-Pfizer monkey virus [19]. Gag is processed by HIV-1 proteinase and the products of the Gag cleavage are: matrix protein (MA - p17), capsid protein (CA - p24), nucleocapsid protein (NC - p7), p6 peptide and two spacer peptides (p2 and p1) (**Figure 1.3**).

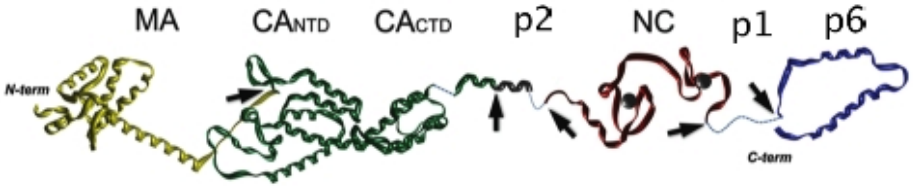

Figure 1.3: Structure of Gag polyprotein with pointed cleavage sites by HIV-1 proteinase. Adopted from [20] and modified.

Matrix protein consists of five α-helices, a short three-β-stranded sheet [21] and the myristic acid moiety attached to N-terminal Gly-residue. It targets Gag to plasma membrane by exposing its myristate moiety to cell membrane. Specific deletion within MA domain leads to disrupted targeting of HIV assembly [22]. Other studies indicate that MA also plays role in Env incorporation to virion during virus budding [23, 24]. In mature virion MA remains associated as a matrix layer within the inner viral membrane.

Capsid consists of two helical folded domains (N-terminal domain - NTD and C-terminal domain - CTD) that are linked by a short linker [25]. CTD contains the major homology

region of Gag which residues stabilize the conformation of the whole domain and thus contributes to Gag-Gag interactions [25, 26]. NTD contains the Cyclophilin A binding site, that packages the prolyl isomerase CypA from the host cell into the virion during virus budding. Preventing CypA incorporation results in disturbed HIV infectivity. It is suggested, that cypA might have function as a chaperone to prevent CA aggregation during maturation [27, 28]. In mature particle, capsid creates the viral core that surrounds HIV genome.

Nucleocapsid contains two zinc-finger motifs Cys-X_2-Cys-X_4-His-X_4-Cys that coordinate zinc ions [29]. These domains participate in RNA binding and encapsidation. NC recognizes a packaging site (ψ site) on the RNA genome and RNA major groove interacts with NC basic residues at positions 3 and 10 [20]. After maturation, nucleocapsid coats the genomic RNA in the viral core [30].

Peptid p6 is a small Pro-rich protein, located at Gag C-terminus. It contains a highly conserved Pro-Thr-Ala-Pro-Pro (PTAP) motif in its L domain, which inactivation leads to impair virion release [31, 32]. The spacer protein p2 controls the viral maturation [33], alteration in its first residues destroys proper viral assembly [34]. The function of p1 is not yet understood [35].

GagPol polyprotein

GagPol polyprotein encodes besides structural proteins (MA, CA, p2, NC) also the transframe protein (TFP) and three enzymes - reverse transcriptase (RT - p66/p51), integrase (IN - p31) and proteinase (PR - p11).

RT is composed of two subunits p66 and p51 that overlap in protein sequence. Domain p66 is derived from GagPol precursor, and after PR cleavage of 15 kDa RNaseH domain, p51 is formed. Although the first residues of amino acid sequence of both subunits are identical, they differ in structural composition. The active site and DNA-binding groove is located in p66, p51 has the structural role [36]. The main role of RT is to transcribe DNA from viral RNA [37]

The IN consists of N-terminal domain with zinc-finger, a central sequence and C-terminal

domain. The active site (Asp64, Asp116 and Glu152) is situated in the central sequence. IN acts as a multimer [38], and incorporates DNA into the host cell genome [39].

HIV-1 PR, which cleaves the Gag and GagPol polyproteins to mature viral components, is discussed in detail in chapter 1.5.

The role of TFP is not clear yet, however, it is the most variable region and the mutations of the viral genome in its gene do influence viral replication and infectivity [40].

Env polyprotein

The polypeptide Env codes the inactive precursor gp160 that is cleaved at the C-terminus of a Lys/Arg-X-Lys/Arg-Arg motif into two envelope proteins gp120 (surface protein - SU) and gp41 (transmembrane protein - TM) [41]. Gp41 anchors Env complex in the viral membrane. The gp120 is noncovalently associated with gp41, and is highly glycosylated [42] which may increase its antigenicity against neutralizing antibodies [43].

Last but not least, HIV-1 encodes six auxiliary proteins Nef, Rev, Tat, Vif, Vpr and Vpu [44]. Tat is the transcriptional transactivator protein that increase the RNA synthesis from HIV-1 LTR. Rev facilitates the transport of viral RNAs from nucleus to cytoplasm. The functions of Vif, Vpr, Vpu and Nef are not completely understood and their detailed analysis are beyond the scope of this thesis [13].

1.3 HIV-1 Assembly and Virion Maturation

The mature viral particle arises through two assembly steps. At first, the cluster of immature Gag is formed around the RNA genome. The Gag molecules are able to interact with envelope polyprotein (Env), which are embedded in the plasma membrane. The capsid in Gag is condensed and it stimulates the coating of lipid bilayer by Env. This results in budding of the immature virion from the cell [45].

The immature virion (**Figure 1.4** on page 17) is a spherical particle with a ranging diameter from 120-260 nm [46]. It consists of a layer of approximately 5000 Gag molecules

associated radially to the inner plasma membrane [47]. Gag precursor is connected to the cell membrane through myristic acid moiety that is joined to N-terminal Gly residue [48]. The C-terminal domain projects to the center of the particle. The Gag lattice is usually open during virus budding and is stabilized by the cell membrane [33].

During the second step, the HIV-1 PR is autoactivated and cleaves Gag and GagPol polyprotein precursors into mature proteins. The autoprocessing is not completely understood, however, one theory claims that it is initiated by dimerization of two HIV-1 PR domains embedded in GagPol precursor [49]. Gag cleavage leads to structural rearrangements and to maturation of the virion.

In the middle of the mature and infectious viral particle (**Figure 1.4**) there is a capsid core with a conical shape. It includes nucleocapsid protein, two molecules of genomic RNA and viral enzymes (reverse transcriptase and integrase). The core is surrounded by lipid bilayer with Env proteins - embedded gp41 and attached gp120. The inner site is covered by MA layer. It is believed that HIV-1 PR is located in the matrix [11, 50].

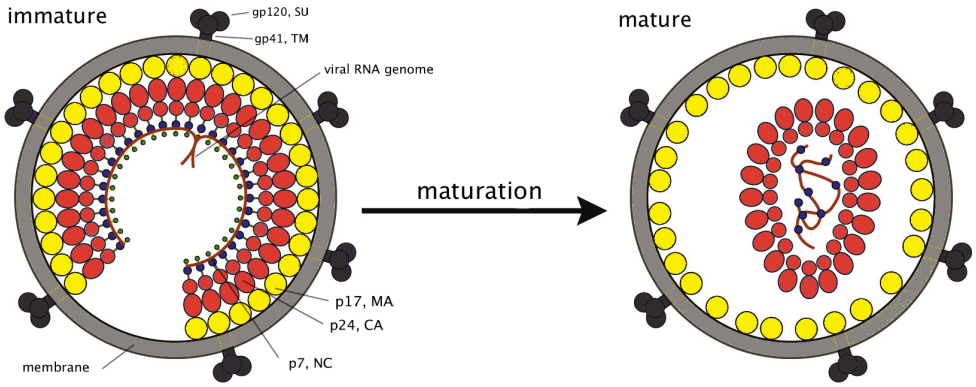

Figure 1.4: The structure of mature and immature HIV particle. Adopted from [47] and modified.

1.4 Current HIV therapy

In 1996, the highly active antiretroviral therapy (HAART) was introduced into clinical practice. It is a combination of 3-4 inhibitors that target viral enzymes. This type of regime helps to slow down the development of the resistance to a specific compound and provides synergism between different drugs, lowering their dosage and side effects. Due to HAART the replication of the virus is suppressed for years, and the quality of people's lives increases [51].

Up to now, the U.S. Food and Drug Administration (FDA) has approved 36 antiretroviral drugs [52]. They may be divided into six categories according to their target in the viral life cycle. For a review, see [51].

The cell entry inhibitors (enfuvirtide, maraviroc) or so called fusion inhibitors interact with receptor proteins on the surface of the cell - the primary receptor CD4+ or coreceptors CCR5 and CXCR4 [53]. The virus is thus unable to bind to the cell membrane and gain entry into the host cell. **Nucleoside Reverse Trascriptase Inhibitors** (abacavir, azidothymidine, didanosine, emtricitabine, lamivudine, stavudine, zalcitabine and zidovudine) are analogues of 2',3'-dideoxynucleoside (ddN). In the cell, they are phosphorylated by three steps into ddNTP and interact with the active site of RT. As a result, they prevent synthesis of DNA and HIV replication. **Nucleotide reverse transcriptase inhibitors** (tenofovir) have the similar effect on the catalytic centre of RT as nucleoside inhibitors. The only difference is in their phosphorylation. **Non-Nucleoside Reverse Transcriptase Inhibitors** (delavirdine, efavirenz, etravirine, nevirapine) are polycyclic compounds that bind to an allosteric site of RT near the active site [54]. **The integrase inhibitor** (Raltegravir) targets the catalytic function of the integrase enzyme, the integration of DNA strand into the host genome [55]. **Proteinase inhibitors** (discussed in chapter 1.5.4) mimic the viral PR substrate. As a result, they suppress the viral maturation [56].

1.5 HIV-1 Proteinase

HIV-1 proteinase (EC 3.4.23.16, 11 kDa) belongs to the family of aspartic proteinases and plays an important role in the late phase of HIV-1 life cycle. It cleaves Gag and GagPol polyproteins at nine sites into structural proteins and enzymes. During this maturation process, the uninfectious viral particle becomes fully infectious.

1.5.1 Structure of HIV-1 Proteinase

HIV-1 proteinase is active as a homodimer consisting of two identical subunits of 99 amino acids [57]. The 3D structure (**Figure 1.5**) was described by multiple studies using crystallographic, NMR and computational analyses [57, 58, 59].

The active site possesses typical catalytic triad of Asp25-Thr26-Gly27 and is formed by catalytic Asp25 of the both subunits at the bottom of the substrate-binding cleft. It is stabilized by hydrogen bonds, between Thr26, Gly27 and catalytic aspartates, that form a network called the fireman's grip. The highly conserved N-terminal residues (1-5) and C-terminal residues (95-99) contribute to dimerization of the enzyme [60]. The structure contains also two β-hairpin loops known as flaps (residues 42-58 and 42'-58'). They are very flexible and allow binding of the substrate or inhibitor to the active site. The flap motion occurs in millisecond–microsecond timescale [61]. The most stable conformation for the enzyme is semi-open [62].

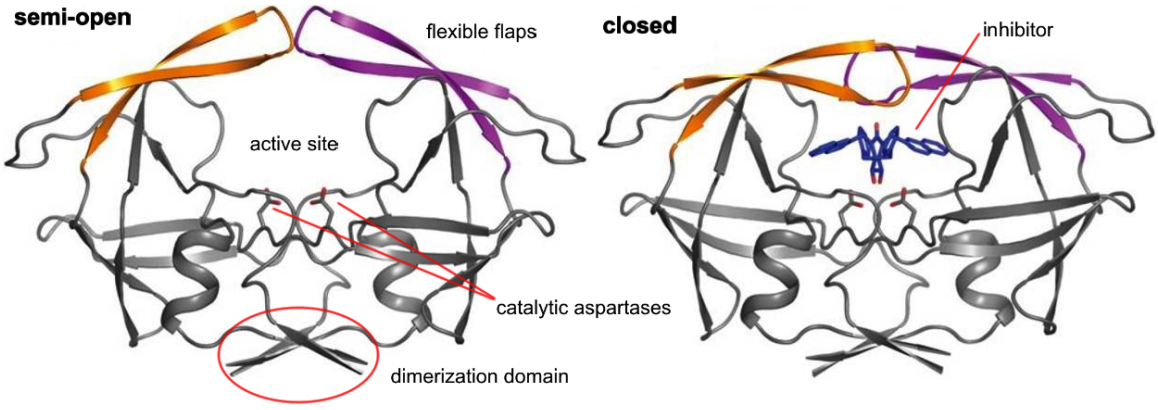

Figure 1.5: The comparison of open and semiopen conformation of HIV-1 proteinase. Flap regions are colored in yellow and purple. Adopted from [62] and modified.

1.5.2 Specificity of HIV-1 Proteinase

HIV-1 proteinase cleaves Gag and GagPol polyproteins at 9 specific sites (**Table 1.1**). HIV-1 PR identifies amino acids of the substrate in the P4 to P3' position, whose side chains interacts with HIV-1 PR subsites, marked as S4 to S3' (**Figure 1.6**) [63]. The shortest substrate is thus 7 amino acids long [64]. There is a preference for two types of processing site - between aromatic amino acid and Pro, or between two hydrophobic amino acids excluding Pro [65]. In type 1, the P2 residue is typically Asn, and P2' is Val/Ile, while in type 2 Glu/Gln is in P2' position [63, 66].

Table 1.1: The sequences of HIV-1 PR cleavage sites. The cleavage occurs between P1 and P1' residues. Adpted from [67].

	P5	P4	P3	P2	P1	P1'	P2'	P3'	P4'	P5'
MA↓CA	V	S	Q	N	Y	P	I	V	Q	N
CA↓p2	K	A	R	V	L	A	E	A	M	S
p2↓NC	P	A	T	I	M	M	Q	R	G	N
NC↓p1	E	R	Q	A	N	F	L	G	K	I
p1↓p6	R	P	G	N	F	L	Q	S	R	P
TF↓PR	V	S	F	N	F	P	Q	I	T	L
PR↓RT	C	T	L	N	F	P	I	S	P	I
RT↓RH	G	A	E	T	F	Y	V	D	G	A
RT↓IN	I	R	K	I	L	F	L	D	G	I

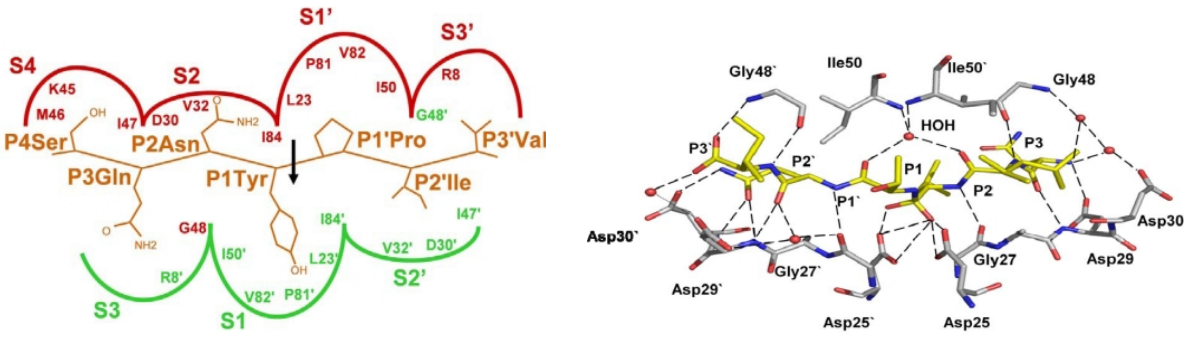

(a) (b)

Figure 1.6: (a) A schematic diagram of the MA↓CA cleavage site. Adopted from [63]. (b) Hydrogen bond interactions of HIV-1 PR with the peptide tetrahedral intermediate. Adopted from [68].

1.5.3 Gag Processing

The cleavage of the Gag polyprotein is a highly regulated sequential process [50]. It happens in a particular order and rate (**Figure 1.7**). The kinetic parameters for each type of cleavage site are shown in **Table 1.2**.

Table 1.2: The kinetic parameters for the wild-type cleavage sites determined via hydrolysis of the respective oligopeptides by the wild-type HIV-1 proteinase. The values were taken from [64, 69] and measured by the same method.

	substrate sequence	K_m (mM)	k_{cat} (s^{-1})	k_{cat}/K_m ($mM^{-1}s^{-1}$)
MA↓CA	VSQNY↓PIVQN	0.15	6.9	46.0
CA↓p2	KARVL↓AEAMS	0.01	0.9	90.0
p2↓NC	PATIM↓MQRGN	0.05	3.7	74.0
NC↓p1	ERQAN↓FLGKI	0.17	0.15	0.9
p1↓p6	RPGNF↓LQSRP	1.20	0.98	0.8

Gag cleavage kinetics was clarified by cell-free expression system of full-length Gag polyprotein [70, 71]. At first, the processing occurs at p2↓NC and it forms two intermediates MA-CA-p2 (41 kDa) and NC-p1-p6 (15 kDa). Then both of the products are cleaved simultaneously at MA↓CA and p1↓p6. The rate is 10-fold lower than the first cleavage. Finally, the spacer peptides p1 and p2 are disconnected from C-termini of NC and CA. These reactions are several hundred-fold slower than the first one and thus they are rate limiting [70]. In particular, the p1↓p6 is 9x slower, MA↓CA 14x slower, NC↓p1 350x slower and CA↓p2 400x slower than the cleavage of p2↓NC [70].

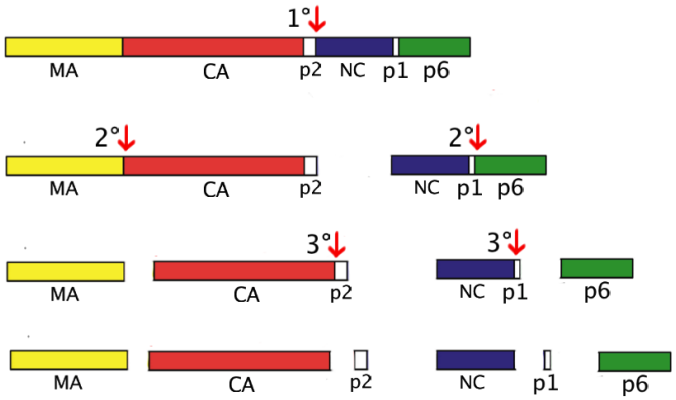

Figure 1.7: Proteolytic processing of Gag polyprotein by HIV-1 PR. The red arrows indicate cleavage sites.

1.5.4 HIV-1 Proteinase Inhibitors

Proteinase inhibitors (PI) (**Figure 1.8** on page 23) used in HIV therapy are tight binding competitive inhibitors that were designed due to detailed knowledge of HIV-1 PR and its specificity. The first generation of PIs are peptidomimetics of the scissile bonds in Gag polyprotein [56]. Unfortunately, they are accompanied with numerous side effects, fast resistance development and low bioavailability. Therefore, the second generation of PIs were developed to overcome these problems. They were designed to inhibit HIV strains resistant to drugs of the first generation. The compounds are much more efficient with improved bioavailability and lowered toxicity and side effects [72, 73].

The first proteinase inhibitor approved by FDA was **saquinavir** (Ro-31-8959, Invirase®) in December 1995 [74]. It was based on specificity of HIV-1 PR to cleave the peptide bond in sequence Asn,Phe↓Pro, which was substituted by a hydroxyethylamine isoester [75]. In 1996, FDA approved another inhibitor called **ritonavir** (ABT-538, Norvir®) [76]. Although, it was developed as C-2 symmetric molecule, it loses symmetry after being bound into the PR active site. More importantly, it is an inhibitor of cytochrome P-450, which is nowadays used in coadministration with other PIs [77]. **Indinavir** (MK-639, L735.524, Crixivan®) was developed on the base of resin inhibitors [78], and approved in 1996. **Nelfinavir** (AG-1343, Viracept®) was licensed in 1997 as the first non-peptidic competitive inhibitor and the first drug approved for children therapy [79].

The scaffold of saquinavir was used to develop the inhibitor **amprenavir** (VX-498, 141W94, Agenerase®) [80], which was approved in 1999. It contains tetrahydrofurancarbamate and sulfonamide moieties. **Fosamprenavir** (VX-175, GW433908, Lexiva®) is a phosphate ester of amprenavir [81], approved in 2003.

In 2000, FDA approved the first inhibitor of the second generation, **lopinavir** (ABT-378, Kaletra®). Its combination with boosting agent ritonavir is used. **Atazanavir** (BMS-232632, CGP 73547, Reyataz®), licensed in 2003, is based on azapeptide analogues [82]. The compound is an once-daily drug with low side effects and good tolerability. The second nonpeptidomimetic inhibitor is **tipranavir** (PNU-140690, Aptivus®) [83], licensed in 2005. Its central scaffold is a dihydropyrone ring unlike a hydroxyethylene core

in peptidomimetic PIs. Although tipranavir has efficacy against several drug resistant strains, it has low tolerability and it is hepatotoxic [84]. It is also CYP450 3A4 inducer, and therefore the therapy requires higher dose of ritonavir. The most recent approved inhibitor (2006) is **darunavir** (TMC-114, UIC-94017, Prezista®). The structure is derived from amprenavir, with replaced tetrahydrofuranyl moiety by bis-tetrahydrofuranyl group [85]. It improves hydrogen bonding and thus its effectivity.

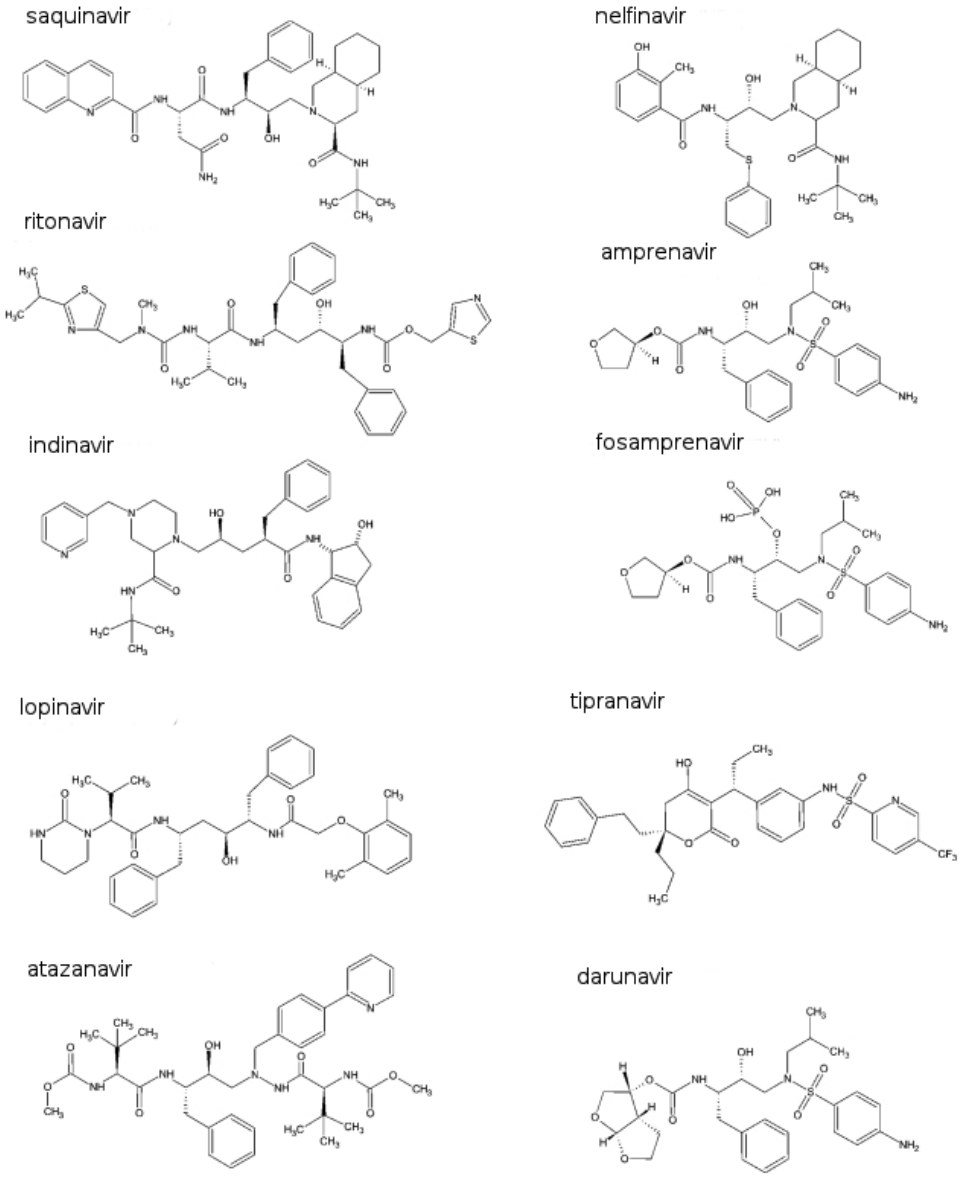

Figure 1.8: Chemical structures of the 1st and 2nd generation of HIV-1 PI. Adopted from [56].

Maturation Inhibitors

The new approach to successfully inhibit the viral maturation, is to employ Gag polyprotein and target its cleavage sites [86]. The disruption of the regulated Gag processing leads to reduced HIV-1 proteinase activity [87]. These specific inhibitors are called maturation inhibitors and represent promising new types of antiretroviral drugs [88].

The prototype of maturation inhibitors is **bevirimat** (PA-457) (3-O-(3'3'- dimethylsuccinyl)betulinic acid - **Figure 1.9**). It is a derivative of betulinic acid, a natural product of plants, which is a weak inhibitor of HIV-1 replication [89]. The derivatization helps to increase the activity of HIV-1 proteinase 1000-fold [90].

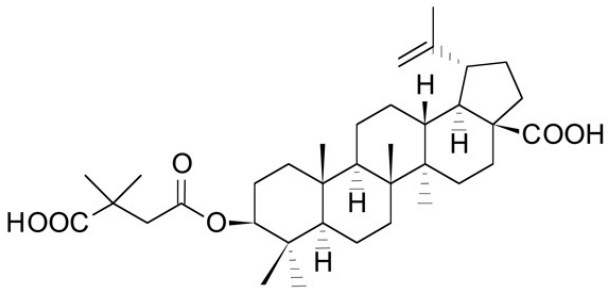

Figure 1.9: The chemical structure of bevirimat. Adopted from [91].

During the virus budding, bevirimat incorporates into HIV virion and associates with the Gag protein in 1:1 stoichiometry [92]. It specifically binds to the cleavage site of CA↓p2 Gag polyprotein and inhibits thus the final rate-limiting step of Gag processing [93, 94]. The major determinants of bevirimat activity are the amino acid residues in N-terminal part of peptide p2 [95]. Bevirimat also has a stabilizing effect on the immature capsid lattice and blocks the conformational transformation of capsid [96]. The disruption of Gag processing and stabilization of capsid results in the formation of abnormal virions with an acentric core and the layer of Gag molecules nearby the plasma membrane [97]. These HIV virus particles remain non-infectious.

Bevirimat is the first maturation inhibitor that has entered the clinical trials [98]. It has an *in vitro* activity against both the wild-type and drug resistant HIV strains, with IC_{50} value around 10 nM [97, 99]. However, mutations conferring to the resistance have already emerged. Bevirimat has high specificity for HIV-1, with no activity against related

retroviruses (HIV-2 and simian immunodeficiency virus) [100].

Other experimental inhibitor in clinical tests is **vivecon** (MPC-9055), which binds within the CA↓p2 junction in Gag and therefore disturbs the proper Gag cleavage [101]. The chemical analogue of bevirimat is a compound called PA1050040, that should represent the second generation of HIV maturation drugs. A third generation inhibitor UK-201844, that target gp160 processing in order to create non-functional Env proteins, is in development [102, 103].

1.5.5 Resistance Development

Although HIV therapy is very effective, the resistance develops to all of the proteinase inhibitors and their combination. The drug-resistant viral species are emerging very quickly, mainly under the selection pressure of PIs. It leads to the rapid viral replication and potential dual infections. The viral reverse transcriptase lacks its proofreading activity, which causes the high mutation rate [56]. The pattern of mutations is very complex, and up to 49 positions in PR amino acid sequence are able to mutate [104]. The resistant mutations within the PR effect the drug susceptibility.

Mutations in HIV-1 Proteinase

The amino acid changes leading to PI resistance (**Figure 1.10** on page 26) are divided into two groups depending on their effect. The **major mutations** are selected early after initiation of the viral therapy, and they are specific to particular inhibitor. Most of them are located in the proximity of the active site of the PR. They frequently affect the processing of the Gag and GagPol polyproteins by enlargement of the catalytic centre of the PR, which leads to weaker interactions between PI and the PR [105].

Later on, the **minor mutations** are selected to improve the viral fitness [105]. They are located outside the substrate-binding cleft.

Although each PI selects different major mutations (**Table 1.3** on page 26), they do overlap and the mutant HIV strain is usually resistant to more than one PI, which is known as cross resistance.

Table 1.3: Positions of resistance mutations in HIV-1 proteinase. Data taken from [106].

PI	Major mutations	Minor Mutations
Amprenavir / Fosamprenavir	50, 84	10, 32, 46, 47, 54, 73, 76, 82, 90
Atazanavir	50, 84, 88	10, 16, 20, 24, 32, 33, 34, 36, 46, 48, 53, 54, 60, 62, 64, 71, 73, 82, 85, 90, 93
Darunavir	47, 50, 54, 76, 84	11, 32, 33, 74, 89
Indinavir	46, 82, 84	10, 20, 24, 32, 36, 54, 71, 73, 76, 77, 90
Lopinavir	32, 47, 76, 82	10, 20, 24, 33, 46, 50, 53, 54, 63, 71, 73, 84, 90
Nelfinavir	30, 90	10, 36, 46, 71, 77, 82, 84, 88
Saquinavir	48, 90	10, 24, 54, 62, 71, 73, 77, 82, 84
Tipranavir	47, 58, 74, 82, 83, 84	10, 33, 36, 43, 46, 54, 69, 89

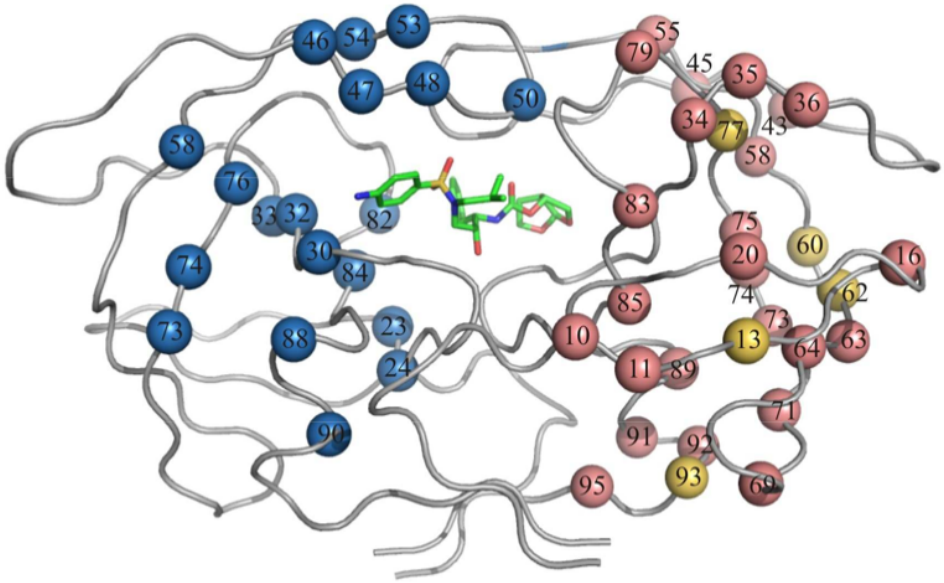

Figure 1.10: 3D structure of HIV-1 proteinase in complex with darunavir. The mutations are shown in one monomer of HIV-1 PR. The major ones are colored in blue, minor in red and polymorphic in yellow. Adopted from [107].

In 0.1 % of patients, amino acid insertions are selected in the lateral edge of the binding cleft [108]. They have been observed ranging from 3 to 18 nucleotides, in PR coding regions near positions 18, 25, 36, 70 and 95 [108]. These inserts are likely created by stalling and slippage of reverse transcriptase. The insertions decrease PI susceptibility, improve viral fitness [109] and contribute to HIV resistance development [110].

Mutations in the Substrate

The mutations within Gag in cleavage sites have been observed both *in vivo* and *in vitro* [111, 112]. These PI resistant variants display improved replicative capacity of the virus.

The mutations in cleavage sites (**Table 1.4**) are most often in the p2↓NC, followed by p1↓p6, NC↓p1, CA↓p2 and MA↓CA [113]. The most frequently selected *in vivo* and *in vitro* mutations are located in amino acid positions 128, 431, 436, 437, 449, 452 and 453. The mutant substrates show higher binding affinity and improved Gag processing by mutant HIV-1 PR. This probably induces the shift in equilibrium of the complex - Gag substrate / proteinase inhibitor with the HIV-1 PR towards the Gag substrate and therefore causes resistance [114].

Table 1.4: Mutations in cleavage sites. Adopted from [114].

Cleavage site										
MA↓CA	V	S	Q	N	Y	P	I	V	Q	N
position	128	129	130	131	132	133	134	135	136	137
variability (%)	3.5	-	4.3	-	3.5	-	-	0.9	0.9	-
substitution	I/T/A/del	-	-	-	F	-	-	-	-	-
CA↓p2	K	A	R	V	L	A	E	A	M	A
position	359	360	361	362	363	364	365	366	367	368
variability (%)	0.2	0.2	1.8	11.5	1.2	-	-	-	-	1.2
substitution	-	V	-	I	M/F/C/Y	-	-	-	-	-
p2↓NC	S	A	T	I	M	M	Q	R	G	N
position	373	374	375	376	377	378	379	380	381	382
variability (%)	36.3	32.6	42.7	23.6	1.8	5.5	-	40.9	5.5	2.1
substitution	P/Q/T	P/S	N/S	V	F	-	-	-	S	-
NC↓p1	E	R	Q	A	N	F	L	G	K	I
position	428	429	430	431	432	433	434	435	436	437
variability (%)	2.3	3.5	-	0.5	-	-	0.1	-	6.3	5.5
substitution	G	-	R	V	-	-	-	-	E/R	T/V
p1↓p6	R	P	G	N	F	L	Q	S	R	P
position	444	445	446	447	448	449	450	451	452	453
variability (%)	-	0.1	-	-	-	9.1	-	22.8	-	8.4
substitution	-	-	-	-	-	F/P/V	-	T/G/R	S/K	A/L/T

The mutations were also identified in non-cleavage sites during PI therapy (**Table 1.5** on page 28). The mechanism of their mediated resistance is, however, not clear. Several of

the amino acid substitutions (L75R, H219Q, V390A/D, R409K and E468K) are resistant to PIs in the presence of PR mutations. [115]. Other (R76K, Y79F, and T81A) reduce PI susceptibility in the absence of PR mutations [116].

Table 1.5: Positions of mutations in Gag precursor protein outside of the cleavage sites. Adopted from [114].

Gag polyprotein	*in vivo*	*in vitro*
MA	76, 79, 81	12, 62, 75, 112
CA	-	200, 219
p2	369, 370, 371	-
NC	389, 401	390, 409
p6	474, 487, 497	468

Although the maturation inhibitor bevirimat is still in clinical studies, several mutations have been identified to confer resistance. They are located at positions 358, 362, 363, 364, 366, 368 and 370 near the CA↓p2 cleavage site [103, 117].

The appearance of mutations in the Gag polyprotein and the possibility to target the cleavage sites suggested to study Gag processing in more detail. Usually the kinetic data were determined using oligopeptides. To obtain proper kinetic characteristic the full-length Gag polyprotein is needed. To determine differences in Gag processing by the wild-type and the mutant variants of HIV-1 PR and to assess the influence of mutations in Gag cleavage sites to HIV resistance are the main goals of this thesis.

Chapter 2

Aims of the Project

The main objective of this thesis was to study Gag processing.
It includes :

- to prepare the full-length recombinant Gag polyprotein
- to determine differences in Gag processing by the wild-type and by highly mutated HIV-1 proteinase
- to assess the influence of mutations in Gag polyprotein on HIV resistance

Chapter 3

Material and Instruments

3.1 List of Chemicals

Table 3.1: Used chemicals

Chemical	Company	Country
2-Mercaptoethanol	Sigma-Aldrich	USA
Acetic acid	Penta	Czech Republic
Acrylamid	USB	USA
Agarose	Bio-Rad	USA
Ammonium persulfate (APS)	Sigma-Aldrich	USA
Ampicillin (AMP)	Biotika	Slovak Republic
Bromphenol Blue	Serva	Germany
Bovine Serum Albumin (BSA)	New England Biolabs	UK
Coommassie Brilliant Blue G250	Serva	Germany
DMSO	Sigma-Aldrich	USA
Ethanol	Lach-Ner	Czech Republic
Ethylenediaminetetraacetic acid (EDTA)	Sigma-Aldrich	USA
Formaldehyde	Lachema	Czech Republic
Glycin	USB	USA

Continued on next page

Table 3.1 – continued from previous page

Chemical	Company	Country
Glycerol	Penta	Czech Republic
Imidazole	Sigma-Aldrich	USA
Isopropyl-β-D-thiogalaktopyranosid (IPTG)	Biosynth Agm	Switzerland
LB - agar	Sigma-Aldrich	USA
LB - medium	Sigma-Aldrich	USA
Methanol	Penta	Czech Republic
Nickel Sulfate	Sigma-Aldrich	USA
Phosphoric Acid	Lachema	Czech Republic
Sodium Acetate	Penta	Czech Republic
Sodium Carbonate (Na_2CO_3)	Penta	Czech Republic
Sodium thiosulphate, pentahydrate ($Na_2S_2O_3.5\ H_2O$)	Penta	Czech Republic
N,N'-methylenbisacrylamide	USB	USA
Silver Nitrate ($AgNO_3$)	LachNer	Czech Republic
Sodium Chloride (NaCl)	Penta	Czech Republic
Sodium Dodecyl Sulfate (SDS)	Sigma-Aldrich	USA
Sodium Sulfite	Lachema	Czech Republic
Sucrose	Fluka	Germany
Tetramethylethylenediamine (TEMED)	Fluka	Germany
Tris(hydroxymethyl)aminoethan (TRIS)	Promega	USA

3.2 Instruments

Autoclave - MLS-3020 U, Sanyo (Japan)

Blotting - Trans - Blot SD Semi-Dry Electrophoresis Transfer Cell, BioRad (USA)

CCD Camera - LAS 3000, Fujifilm Corporation (Japan)

Centrifuges - Allegra X-15 R (Beckman Coulter), Avanti J-30 I (Beckman Coulter)
- Beckman J2-MI, Beckman Coulter (USA)
- Eppendorf centrifuge 5415R, Eppendorf (Germany)

Chromatography - AKTA explorer, Amersham Pharmacia Biotech (Sweden)

Electrophoresis - Horizontal electrophoresis apparatus, Shelton Scientific (USA)
- Vertical polyacrylamid electrophoresis, Amersham Pharmacia Biotech (Sweden)

Emulsiflex - Emulsiflex C-3 microfluidizer, Avestin (Germany)

pH Meter - Unicam 9450, Unicam (UK)

Rotary Incubator - Innova 44, New Brunswich Scientific (Germany)

Shaker - KS 260 basic shaker, IKA (Germany)

Spectrophotometers - UV-VIS Spectrophotometer UNICAM UV 500, Unicam (UK)
- UV- VIS Spectrophotometer SPECORD 210, Analytik Jena (Germany)

Transilluminators - UV Transilluminator, UltraLum (USA)
- Safe Imager Blue Light Transilluminator, Invitrogen (The Netherlands)

Thermal Cycler - Techne Progene Thermocycler (UK)

3.3 Other Used Materials

Bacterial strains and vectors - *E.coli* DH5α, *E.coli* BL21(DE3)RIL, Novagen (USA)

- pET22b (AMP+), Novagen (USA)

Blotting - anti-capsid antibody (monoclonal, rabbit, lab of Hans-Georg Kräusslich)

- anti-matrix antibody (monoclonal, rabbit, lab of Jan Weber)
- PVDF membrane, Millipore (USA)
- SuperSignal West Femto Chemiluminescent Substrate, Pierce (USA)

Columns - Superdex 200 GL, GE Healthcare (UK)

- HiTrap^{TM} Chelating HP columns, GE Healthcare (UK)

Enzymes - *Phusion* DNA Polymerase, T4 DNA Ligase, New England Biolabs (UK)

- restriction endonuclease : *XhoI*, Takara (Japan), *NdeI*, New England Biolabs (UK)
- drv6 HIV-1 proteinase (Prepared by Klára Grantz Šašková at IOCB AS CR)
- oligonucleotide primers, East Port (Czech Republic)

Filtration - Sterivex 0.22 μm Filter Unit, Millipore (USA)

Kits - Gel/PCR DNA fragments Extraction kit, Geneaid (Taiwan)

- High-Speed Plasmid Mini Kit, Geneaid (Taiwan)

Solutions - NEBuffer 4, T4 DNA buffer, GC buffer, New England Biolabs (UK)

- PPP Master Mix solution, TopBio (Czech Republic)
- Ethidium Bromide, Sigma-Aldrich (USA)
- SYBR Safe DNA gel stain, Invitrogen (The Netherlands)

Standards - MW standard - All Blue, BioRad (USA)

- 1 kb DNA ladder, New England Biolabs (UK)

Other materials - Darunavir, Tibotec, BVBA (USA)

- Chromogenous substrate KARVNIe$\downarrow$NphEANIe-NH_2 (Prepared by Mirka Blechova at IOCB AS CR)
- Proteinase Inhibitor cocktail tablets, Roche (Switzerland)

Chapter 4

Methods

4.1 Cloning of Fusion Variants of Gag Polyprotein

The gene encoding the Gag polyprotein either with or without N-terminal poly-His-tag was amplified by PCR reaction (**Table 4.1A** on page 35). The forward primers (Gag fw, HisGag fw) containing the cleavage site for *EcoRI* (GAATTC) and *NdeI* (CATATG) were specific to the 5'-end of the Gag coding region and the reverse primer (Gag rv) was specific to 3'-end of the Gag coding region.

The MBP region (with and without C-terminal poly-His-tag) was amplified by PCR reaction (**Table 4.1B** on page 35) using a forward primer (MBP fw) containing cleavage site for TEV proteinase (GAAAACCTGTACTTCCAGTCT) specific to 3'-end of MBP coding region and reverse primer (MBP rv, MBPHis rv) with cleavage site for *XhoI* (CTCGAG), specific to 3'-end of the MBP coding region .

All the primers were synthesized by East Port (CZ) and used in concentration of 20 μM. The PCR reactions were performed as follows:

1. 98 °C / 10 min
2. (98 °C / 30 s, 52 °C / 30 s, 72 °C / 180 s) 30 cycles
3. 72 °C / 8 min

The products were isolated from 1.2 % agarose gel (chapter 4.1.2) and fused together in the second PCR reaction (**Table 4.1C** on page 35). The time of elongation step was

Table 4.1: Sequence of PCR reactions used in preparation of DNA inserts.

product		templates	primers	dNTPs	PhuPol	DMSO	GC b.	H_2O
Gag-MBP	A	Gag (5 μl)	1, 2 (1 μl)	1 μl	0.5 μl	1.5 μl	10 μl	30 μl
	B	MBP (5 μl)	3, 4 (1 μl)	1 μl	0.5 μl	1.5 μl	10 μl	30 μl
	C	A, B (10 μl)	-	1 μl	0.5 μl	1.5 μl	10 μl	17 μl
	D	C (1 μl)	1, 4 (1 μl)	1 μl	0.5 μl	1.5 μl	10 μl	34 μl
HisGag-MBP	A	Gag (5 μl)	5, 2 (1 μl)	1 μl	0.5 μl	1.5 μl	10 μl	30 μl
	B	MBP (5 μl)	3, 4 (1 μl)	1 μl	0.5 μl	1.5 μl	10 μl	30 μl
	C	A, B (10 μl)	-	1 μl	0.5 μl	1.5 μl	10 μl	17 μl
	D	C (1 μl)	5, 4 (1 μl)	1 μl	0.5 μl	1.5 μl	10 μl	34 μl
Gag-MBPHis	A	Gag (5 μl)	1, 2 (1 μl)	1 μl	0.5 μl	1.5 μl	10 μl	30 μl
	B	MBP (5 μl)	3, 6 (1 μl)	1 μl	0.5 μl	1.5 μl	10 μl	30 μl
	C	A, B (10 μl)	-	1 μl	0.5 μl	1.5 μl	10 μl	17 μl
	D	C (1 μl)	1, 6 (1 μl)	1 μl	0.5 μl	1.5 μl	10 μl	34 μl

Notes: Phusion Polymerase (PhuPol - 2000 U/ml)
Primer 1 (Gag fw) 5'-ATCGAATTCATATGGGTGCGAGAGCGTCG-3'
Primer 2 (Gag rv) 5'-AGACTGGAAGTACAGGTTTTCTTGTGACGAGGGGTCGCTGCC-3'
Primer 3 (MBP fw) 5'-GAAAACCTGTACTTCCAGTCTAAAATCGAAGAAGGCAAACTG-3'
Primer 4 (MBP rv) 5'-ACGGATCCTCGAGCTATTTGGTGATACGGGTCTG-3'
Primer 5 (HisGag fw) 5'-ATCGAATTCATATGCACCACCACCACCACCACGGTGCGAGAGCGTCGGTA3'
Primer 6 (MBPHis rv) 5'-ACGGATCCTCGAGTTTGGTGATACGGGTCTG-3'

extended from 180 s to 210 s. The products were amplified in the third PCR reaction (**Table 4.1D**), in which the temperature of elongation step was 65 °C and time 210 s.

The purified PCR product was digested with two restriction endonucleases *NdeI* and *XhoI*. The digestion reaction contained 10 μl of PCR product, 2 μl of NEB buffer 4, 2 μl of BSA (10x), 0.5 μl of *NdeI* (20000 U/ml), 0.5 μl of *XhoI* (5000 U/μl) and 5 μl of sterile H_2O. The reaction mixture was left overnight at 37 °C. Digested enzymes were denatured at 65 °C for 20 min.

Isolated DNA was ligated into the expression vector pET22b. The reaction mixture contained 10 μl of isolated DNA, 1 μl of plasmid, 2 μl of T4 DNA ligase buffer (10x), 0.5 μl of T4 DNA ligase (400000 U/ml) and 6.5 of sterile μl H_2O. The ligation proceeded 4 h at laboratory temperature.

The ligation inserts were sequenced in DNA Sequencing Laboratory, Faculty of Science, Charles University in Prague.

4.1.1 Horizontal Agarose Gel Electrophoresis

TAE buffer (50x) - 2 M Tris, 1 M Acetic Acid, 50 mM EDTA, pH 8.0
Sample buffer - 40 % (w/v) sucrose, 0.1 % (w/v) bromphenol blue

DNA fragments were analyzed by horizontal agarose gel electrophoresis. To prepare 1.2 % gel, 0.72 g agarose was dissolved in 60 ml of TAE buffer (1x). The suspension was heated in microwave oven until agarose melted and the evaporated water was refilled. After cooling down, the fluorescent indicator ethidium bromide (60 μl of 0.5 mg/ml) was added and the gel was poured into the casting platform and the comb was inserted. Solidified gel was transferred to the electrophoresis apparatus filled with TAE buffer (1x). The DNA samples mixed with the sample buffer were loaded to the gel and electrophoresis ran at constant voltage of 110 V / 40 min. The ethidium bromide-stained DNA was visualized using ultraviolet transilluminator. When DNA was isolated from the agarose gel, the 6 μl SYBR safe DNA gel stain (10000x diluted) was added to gel solution instead of ethidium bromide. This gel was visualized with blue light transilluminator.

4.1.2 DNA Isolation from Agarose Gel

DNA fragments were isolated using Geneaid Gel/PCR DNA fragments Extraction kit according to the manufacturers instuctions. Gel slice (300 mg) with relevant DNA was dissolved in 500 μl of DF buffer and the suspension was incubated at 60 °C for 10 min. After cooling down, the sample was transferred to collection tube and centrifuged (14000 g, 30 s) in order to bind DNA to the membrane. It was washed with 400 μl of W1 buffer by centrifugation (14000 g, 30 s) and with 600 μl of Wash buffer by centrifugation (140000 g, 30 s), and spinned down again to dry the column matrix. Dried column was transferred into a new microtube, and 30 μl of Elution buffer was added to the center of the column matrix. It was left for 2 minutes, and then the purified DNA was eluted by centrifugation (14000 g, 2 min).

4.1.3 Transformation of Bacterial Cells

To prepare agar plates, LB agar (8.75 g) was dissolved in water (250 ml) and sterilized at 121 °C for 15 minutes by autoclave. Ampicillin was added to the final concentration of 0.1 mg/ml and 10 ml of this solution was poured on the sterile Petri plate.

The ligation product (20 μl) was added to 100 μl of competent cells *Escherichia coli* DH5α. It was left 30 min on ice, 90 s in 42 °C (heat shock) and 120 s on ice. It was followed by cell incubation with 300 μl of sterile medium at 37 °C for 1 h. The cells were plated on the prepared agar plates and incubated overnight at 37 °C.

4.1.4 Isolation of the Plasmid DNA

Single colony grown on LB agar plates was picked and transferred into 5 ml of sterile LB medium with ampicillin (1000x). The bacterial inoculum was incubated in rotary incubator overnight at 37 °C, and the plasmid DNA was isolated from the cultured bacterial cells using High-Speed Plasmid Mini Kit according to the manufacturers instructions. Grown bacterial culture was centrifuged at 14000 g for 1 min and resuspended in 200 μl of PD1 buffer containing RNase A. 200 μl of PD2 buffer was added, gently mixed and left at room temperature until the lysate was homogeneous. Lysate was neutralized by the addition of 300 μl of PD3 buffer, stirred and centrifuged (14000 g, 3 min). The supernatant was transferred into the PD column and centrifuged (14000 g, 30 s). The bound DNA was washed with 400 μl of W1 buffer by centrifugation (14000 g, 30 s) and with 600 μl of Wash buffer by centrifugation at the same conditions. The column matrix was dried by centrifugation at 14000 g for 3 min and then 50 μl of Elution buffer was added into its center. DNA was eluted by centrifugation (14000 g, 2 min).

4.2 Protein Expression

Lysis buffer A - 50 mM Tris, 50 mM NaCl, 1 mM EDTA, pH 8.0

Competent cells *E. coli* BL21(DE3)RIL (50 μl) were transformed by the expression vector coding the Gag polyprotein (2 μl). The transformation was carried out as in chapter 4.1.3.

Freshly grown colonies on agar plates were resuspended in 12 ml of LB medium and inoculated in 500 ml of sterile LB medium supplemented with AMP (100 μg/ml). They were grown in a rotary incubator at 37 °C, 220 rpm. After reaching the OD_{595} value of 0.7, the expression was induced by addition of IPTG to final concentration of 0.75 mM. The cells were incubated for 3 h at the same conditions and then centrifuged (20 000 g, 10 min, 25 °C). The pellet was weighed and resuspended in the lysis buffer A (10 ml of buffer A per 1 g of wet biomass).

Only the product HisGag-MBP was used in the following experiments. The expression conditions were the same, the production was, however, carried out in 6 x 500 ml of sterile LB medium with AMP (100 μg/ml). After pelet resuspension in lysis buffer, one tablet of the proteinase inhibitor cocktail (Roche) was added and it was frozen in -80 °C for later use.

4.3 Protein Isolation and Purification

Thawed solution was three times homogenized using Potter homogenizer and then the cells were lysed three times via Emulsiflex using homogenizing pressure set to 10000-15000 psi. The lysate was centrifuged at 10000 g, 20 min, 4 °C and the supernatant was filtered through a 0.22 μm syringe filter.

4.3.1 Immobilized-metal Affinity Chromatography

Buffer A - 20 mM Tris, 0.1 % 2-mercaptoethanol, pH 8.0

Buffer B - 20 mM Tris, 0.1 % 2-mercaptoethanol, 500 mM imidazole, pH 8.0

To purify the His-tag protein the immobilized-metal affinity chromatography (IMAC) was used. It is based on affinity of Ni^{2+} metal ion to histidine residues of the His tag. The purification proceeded on 2 HiTrap^{TM} Chelating HP columns (1 ml volume) attached to the AKTA Explorer liquid chromatography system. The column was charged with 0.1 M nickel sulfate.

During the protein purification, the flow rate was 1 ml/min. The column was equilibrated with the buffer A and then the protein sample was loaded. It was subsequently washed with buffer A and the bound proteins were eluted by a gradient of 0-5 % of buffer B in 10 min and 5-100 % of buffer B in 20 min. The protein concentration in eluates during the procedure was monitored by Bradford assay (chapter 4.4.1). Protein fractions were analyzed by SDS electrophoresis (chapter 4.4.2).

4.3.2 Gel Permeation Chromatography

Buffer B - 20 mM Tris, 0.1 % 2-mercaptoethanol, 500 mM imidazole, pH 8.0

Gel permeation chromatography (GPC) was used to fractionate the protein based on the size. The elution fractions from IMAC were loaded on the column Superdex 200 equilibrated with buffer B. The flow rate was 0.4 ml/min and the purification was monitored by on-line absorbance measurement at 280 nm. After protein separation, the peak fractions were analyzed by SDS electrophoresis (chapter 4.4.2), and the protein concentration was determined by Bradford analysis (chapter 4.4.1). The fractions containing purified protein HisGag-MBP were pooled and stored at -80 °C.

4.4 Protein Analysis

4.4.1 Determination of Protein Concentration

Commassie blue G-250 solution - 100 mg Commassie brilliant blue G-250, 50 ml 96 % ethanol, 100 ml 85 % phosphoric acid, 850 ml sterile water

The protein concentration was determined using the Bradford method [118]. The samples contained a range of 15 - 100 μl of protein, 200 μl of Coomassie Brilliant Blue G-250 and sterile water was added to a total volume of 1 ml. The samples were incubated for 5 min at laboratory temperature, the absorbance at 595 nm was analyzed and the value of protein concentration was established from the calibration curve of Bovine serum albumin (BSA).

4.4.2 SDS - Polyacrylamid Gel Electrophoresis

Sample buffer (6x) - 3.5 ml 1M Tris, 3 ml glycerol, 1 g SDS, 600 μl 2-mercaptoethanol, 1.2 mg bromphenol blue, water to 10 ml, pH 6.8
Electrode buffer - 25 mM Tris, 250 mM glycin, 0.1 % (w/v) SDS
44 % polyacrylamide solution (AAmix) - 42.8 g acrylamide, 1.2 g N,N'-methylenbisacrylamide, water to 100 ml

The protein isolation and purification steps were monitored by discontinuous Sodium Dodecyl Sulphate Polyacrylamide Gel Electrophoresis (SDS-PAGE). The samples were separated using a 6.6 % stacking gel and 10 % or 18 % separating gel, prepared as described in **Table 4.2** on page 41.

The samples were mixed with the sample buffer in the ratio of 5:1 and they were denatured by boiling for 5 min. The commercial standard All Blue was used to determine molecular weight. Electrophoresis was carried out at constant voltage of 140 V, 1 h. Separated proteins were stained by silver (**Table 4.3** on page 41).

Table 4.2: The preparation of polyacrylamide gels

	separating gel (10 %)	separating gel (18 %)	stacking gel (6.6 %)
1.5 M Tris-HCl	2.5 ml	2.5 ml	1.25 ml
44 % AAmix	2.3 ml	4 ml	750 μl
10 % (w/v) SDS	100 μl	100 μl	50 μl
TEMED	10 μl	10 μl	10 μl
10 % APS	100 μl	50 μl	50 μl
sterile water to	10 ml	10 ml	5 ml

Table 4.3: Silver staining of proteins on SDS-PAGE

step	solution	time
1	12 % (v/v) acetic acid, 50 % (v/v) methanol, 0.02 % (v/v) formaldehyde	30 min
2	50 % (v/v) methanol	3 x 15 min
3	$Na_2S_2O_3.5\ H_2O$ (0.2 g/l)	1 min
4	sterile water	3 x 20 s
5	$AgNO_3$ (2 g/l), 0.02 % (v/v) formaldehyde	20 min
6	sterile water	3x 20 s
7	Na_2CO_3 (60 g/l), $Na_2S_2O_3.5H_2O$ (4 g/l), 0.02 % (v/v) formaldehyde	until bands appear
8	sterile water	3 x 20 s
9	12 % (v/v) acetic acid, 50 % (v/v) methanol	10 min
10	10 % (v/v) acetic acid	overnight

4.4.3 Western Blotting

Blotting concentrate - 72.1 g glycine (1.92 M), 15.1 g Tris (250 mM), water to 500 ml
Blotting buffer - 10 ml blotting concentrate, 8 ml methanol, 1 ml 10 % (w/v) SDS, water to 100 ml
Blocking buffer - 3 % Bovine Serum Albumin (BSA) (w/v) in PBS

The proteins separated by SDS electrophoresis gel were transferred to a polyvinylidene difluoride (PVDF) membrane. The polyacrylamide gel, PVDF membrane and filter papers were equilibrated in blotting buffer and placed on the transfer apparatus in the following order (from anode to cathode) : 2x filter paper - PVDF membrane - polyacrylamide gel - 2x filter paper. The transfer was performed at constant voltage of 15 V for 15 min.

The membrane was blocked in 5 ml of blocking buffer for 1 h, and then incubated with primary anti-capsid antibody (rabbit, 1:1000) overnight at 4 °C. Membrane was washed three times by PBS + 0.05 % Tween-20 and then was complexed with secondary HRP-conjugated antibody (anti-rabbit) for 1 h at 4 °C. The membrane was washed again by PBS + 0.05 % Tween-20 and incubated with SuperSignal West Femto Chemiluminescent Substrate. The chemiluminiscence signal was captured using CCD camera.

After developing the blot, the membrane was washed three times in PBS and then incubated in 5 ml of stripping buffer (Pierce, USA) for 15 min. It was washed again, and the primary anti-matrix antibody (rabbit, 1:3000) was added. The Western blotting proceeded as before.

4.5 Kinetic Measurements

4.5.1 Determination of Kinetic Constants

Reaction buffer - 2 mM Tris, 50 mM imidazole, 500 mM sodium acetate, 0.01 % 2-mercaptoethanol, pH 4.63

The kinetic parameters were determined for the wild-type HIV-1 proteinase as well as the mutated drv6 HIV-1 PR. This variant, that was selected as a representative mutant of HIV-1 PR, contains amino acid exchanges L10I, I13V, I15V, K20R, L33F, E34N, E35D, M36I, K43T, I47V, I50L, F53L, Q58E, I62V, L63P, I66F, A71V, V77I, V82A, I84V, L89V. It was purified in our laboratory by Grantz Šašková et al. [119].

The spectrophotometric assay employed the chromogenic peptide substrate KARVNIe↓NphEANIe-NH_2 (Nle is norleucine, Nph is p-nitrophenyl-alanine), which was derived from the cleavage site Ca↓p2 in Gag polypeptide. The decrease in absorbance at 305 nm caused by CA↓p2 cleavage was observed, and the shift in 1 ml of reaction mixture at 37 °C in 1 cm cuvettes was monitored using an UV/VIS spectrophotometer.

Michaelis-Menten constant K_m and the maximum rate V_{max} were determined from the measurement of initial rate (v_0) of the substrate cleavage (15 μM) by the wild-type proteinase (9 nM) and by increasing the substrate concentrations with constant PR concentration. The data were analyzed according to Michaelis-Menten equation **4.1**.

$$v_0 = \frac{V_{max} * [S]}{K_m + [S]} \tag{4.1}$$

where v_0 is the initial rate of the reaction, V_{max} is the limit reaction rate, K_m is Michaelis-Menten constant and [S] is concentration of the substrate.

The catalytic efficiency k_{cat} was determined by transforming all the substrate (10.5 μl, 3.31 mM) by 3 μl of PR (15.1 μM) in the reaction, and calculated from the equation **4.2**.

$$k_{cat} = \frac{V_{max}}{[E]_0} = \frac{V^A_{max} * [S_0]}{[E]_0 * \Delta A} \tag{4.2}$$

where V^A_{max} is the maximum velocity expressed as the absorbance decrease per unit of time, $[E_0]$ is the total enzyme concentration in the cuvette, $[S_0]$ is the enzyme concentration in the reference experiment in which its total cleavage by PR was facilitated, and ΔA is the corresponding change in absorbance.

The same principles were used to determine kinetic parameters for drv6 HIV-1 PR in the same reaction buffer. The final concentration of drv6 in all reactions was 8.3 nM.

4.5.2 Kinetics of Gag Processing

Stock buffer (10x) - 5 M Sodium Acetate, pH 4.4

The obtained protein HisGag-MBP was cleaved by either the wild-type HIV-1 proteinase (10 nM) or mutated HIV-1 PR - variant drv6 (10 nM).

The substrate cleavage was performed in several reaction mixtures (**Table 4.4**). The kinetics was observed in 24 hour interval. All the reactions proceeded at laboratory temperature and they were stopped by adding 4 μl of Sample buffer from SDS-PAGE and boiled in 100 °C water for 5 s. Two negative controls were used, one without HIV-1 PR and another with the addition of HIV-1 PR inhibitor darunavir (drv - 30 nM). The Gag processing was analyzed by SDS-PAGE and Western blotting using anti-capsid and anti-matrix antibodies.

The Gag processing was also observed by cleavage with mutated HIV-1 proteinase drv6, that was used in the same concentration as the wild-type PR. The cleavage conditions remained the same.

Table 4.4: The cleavage experiments

		time	S (200 nM)	PR (10 nM)	H_2O	stock b.	drv
SDS-PAGE	samples	0,1,5,10,24 h	4 μl	0.8 μl	4.2 μl	1 μl	-
	control 1	24 h	4 μl	-	5 μl	1 μl	-
	control 2	24 h	4 μl	0.8 μl	3.4 μl	1 μl	0.8 μl
Western blotting	samples	0,1,5,10,24 h	2 μl	0.4 μl	6.6 μl	1 μl	-
	control 1	24 h	2 μl	-	7 μl	1 μl	-
	control 2	24 h	2 μl	0.4 μl	6.2 μl	1 μl	0.4 μl

Chapter 5

Results

5.1 Preparation of Individual DNA Constructs of Gag Polyprotein

Three Gag variants designed within this diploma thesis are schematically shown in **Figure 5.1**. They were marked as Gag-MBP, HisGag-MBP and Gag-MBPHis according to N- or C-terminal poly-His-tag and maltose binding protein (MBP).

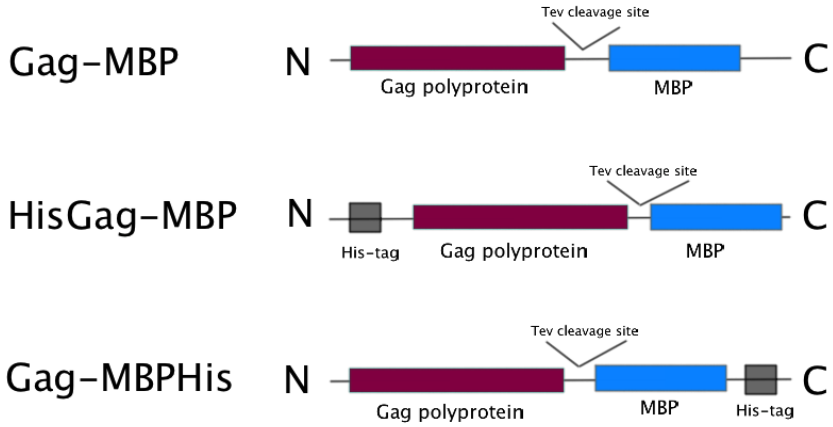

Figure 5.1: Scheme of prepared Gag variants.

DNA sequence of the variant Gag-MBP is shown in **Figure 5.2** on page 46. At first, the Gag (MBP) sequence was amplified using Gag fw and Gag rv primers (MBP fw, MBP rv) (**Figure 5.3a** on page 46). After DNA isolation, the target fragments (Gag - 1521 bp

and MBP - 1110 bp) were joined in second PCR reaction and the yield of the fused product was increased by the third round of PCR reactions (**Figure 5.3b**).

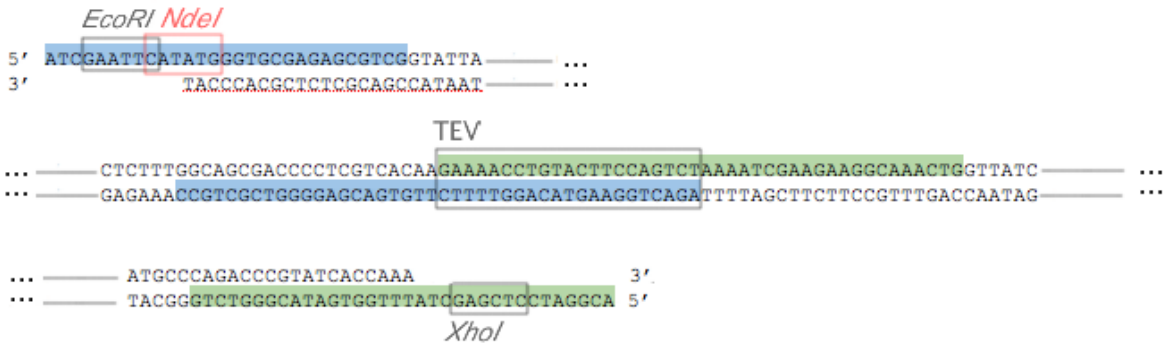

Figure 5.2: DNA sequence of Gag-MBP with pointed cleavage sites for restriction enzymes. The sequence of primers are highlighted in blue (Gag fw, Gag rv) and green (MBP fw, MBP rv).

The isolated final products were cleaved by restriction enzymes *NdeI* and *XhoI* and ligated into the pET22b expression vector. *E.coli* DH5α cells were transformed by ligation product (chapter 4.1.3) and the DNA minipreparations were carried out (chapter 4.1.4). The successful ligation was confirmed by restriction cleavage on agarose gel electrophoresis (**Figure 5.4** on page 47). Sequence analysis of the inserts confirmed the correct clones.

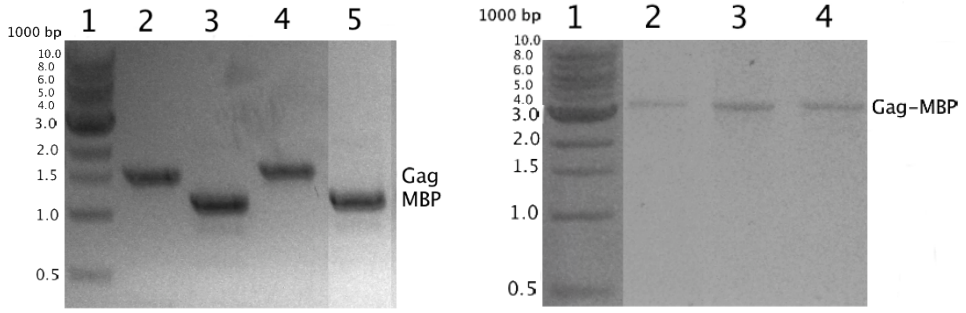

(a) (b)

Figure 5.3: Agarose gel electrophoresis. (a) The *gag* and *mbp* genes amplified by PCR reaction. *Lane 1*: 1kb DNA ladder, *lane 2*: gag (primers 1,2), *lane 3*: MBP (primers 3,4), *lane 4*: HisGag (primers 5,2), *lane 5*: MBPHis (primers 3,6) (b) Fused products. *Lane 1*: 1kb DNA ladder, *lane 2*: Gag-MBP, *lane 3*: HisGag-MBP, *lane 4*: Gag-MBPHis. In both gels, the irrelevant lanes were omitted for clarity.

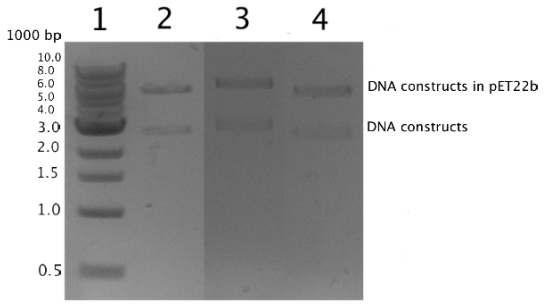

Figure 5.4: The agarose electrophoresis confirming the presence of the DNA fragment encoding the GagMPB in plasmid pET22b. *Lane 1*: 1kb DNA ladder, *lane 2*: Gag-MBP, *lane 3*: HisGag-MBP, *lane 4*: Gag-MBPHis. The irrelevant lanes on the gel were omitted.

5.2 Test of Recombinant Expression of Individual Gag Variants

The competent cells *E.coli* BL21(DE3)RIL were transformed by all three protein variants. The cultures were grown at 37 °C for 4 h in 0.5 l of LB media with ampicillin and the recombinant expression was induced by adding IPTG to final concentration of 0.75 mM. After 3 h of incubation, the cells were harvested and the pellet was weighted: 2.9 g of wet biomass was pelleted by centrifugation of protein Gag-MBP, 2.9 g by HisGag-MBP and 1.8 g by Gag-MBPHis per 0.5 liter of culture. The cells were resuspended in the lysis buffer A and disrupted at 4 °C using emulsiflex. All of the fractions were analyzed on 18 % SDS-PAGE gel (**Figure 5.5a** on page 48).

5.3 Upscaled Recombinant Expression of HisGag-MBP

The *E.coli* BL21(DE3)RIL strain was transformed by the DNA coding the HisGag-MPB variant, and the cells were grown in 6 x 0.5 l of LB media. The bacterial growth was monitored by measuring OD_{595} as shown in **Figure 5.6** on page 48. When OD_{595} reached the value of 0.7, the expression was initiated by addition of IPTG to a final concentration of 0.75 mM. The cells were lysed and the collected fractions were analyzed on 18% SDS-PAGE gel (**Figure 5.5b** on page 48). The cells overexpressing HisGag-MBP variant contained a large amount of soluble protein, which was subsequently used for further purification.

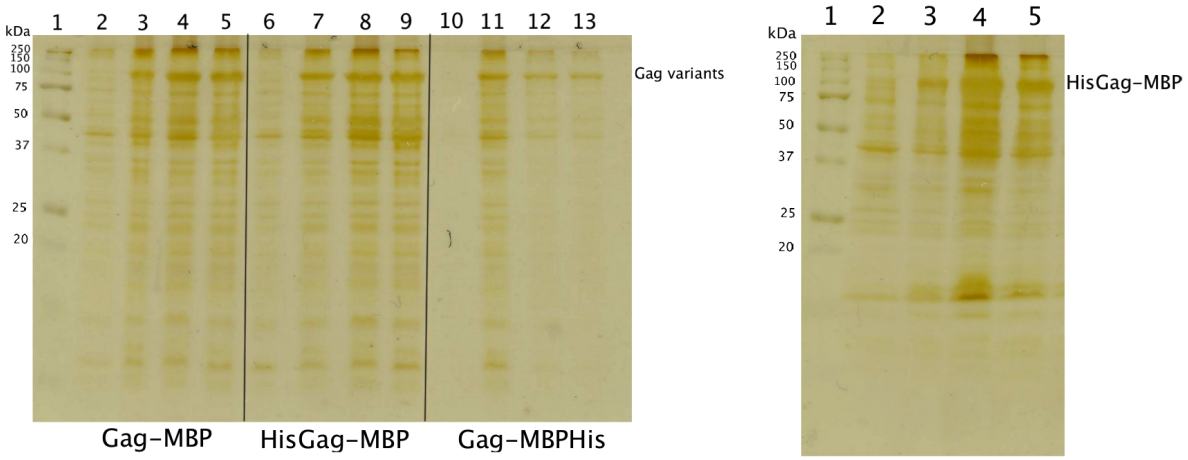

(a) (b)

Figure 5.5: (a) 18 % SDS-PAGE showing the expression of protein variants. *Lanes 2-5*: Gag-MBP, *lanes 6-9*: HisGag-MBP and *lanes 10-13*: Gag-MBPHis, *lane 1*: MW standard, *lanes 2, 6, 10*: bacterial cells before induction, *lanes 3, 7, 11*: bacterial cells after induction, *lanes 4, 8, 12*: bacterial cells after cell lysis, *lanes 5, 9, 13*: supernatant after cell lysis. (b) The upscaled expression of HisGag-MBP. *Lane 1*: 1kb DNA ladder, *lane 2*: bacterial cells before induction, *lane 3*: bacterial cells after induction, *lane 4*: bacterial cells after cell lysis, *lane 5*: supernatant after cell lysis.

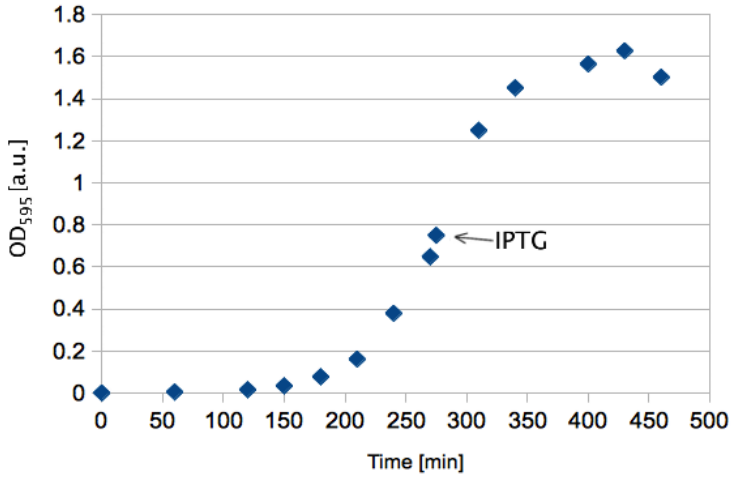

Figure 5.6: The growth curve of *E.coli* BL21(DE3)RIL transformed with HisGag-MBP expression vector. When OD_{595} reached the value of 0.7, the expression was induced by 0.75 mM IPTG.

5.4 Purification of HisGag-MBP

Immobilized-metal affinity chromatography was employed for purification of His-tagged protein HisGag-MBP. The column was precharged with Ni^{2+}, equilibrated with buffer A and the cell lysate was loaded on the column. The trapped protein was eluted by gradient of 500 mM imidazole (chapter 4.3.1). The process of elution is seen in **Figure 5.7**. A considerable portion of HisGag-MBP (lane 2) runs through the column without binding (lane 3), and some of HisGag-MBP protein was washed away (lane 4). Bound HisGag-MBP protein (97 kDa) was eluted in fractions 8-10 and in end-fraction containing 100 % of buffer B (lane 10).

The eluted fractions (8, 9, 10 and 100 %) were collected, pooled and purified using GPC chromatography in 3 portions due to limited column capacity (chapter 4.3.2). The buffer contained 500 mM imidazole to stabilize the protein during purification. The eluted fractions were analyzed on 10 % SDS gel (one of three rounds **Figure 5.8** and **Figure 5.9** on page 50). All the fraction containing HisGag-MBP were collected and the concentration was analyzed (chapter 4.4.1). The final yield of the HisGag-MBP protein was 1 mg/l of LB media. Total amount of the protein was 4 mg.

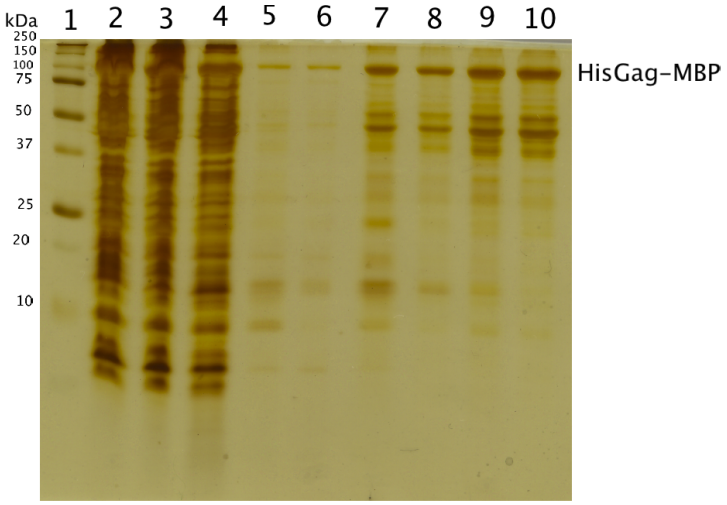

Figure 5.7: 18 % SDS PAGE gel showing protein purification using IMAC. *Lane 1*: MW standard (1 μl), *lane 2*: load (3 μl), *lane 3*: flow through (3 μl), *lane 4*: wash 1 (3 μl), *lane 5*: wash 2 (3 μl), *lane 6*: 0-5 % of buffer B (3 μl), *lanes 7, 8, 9*: 5-100 % of buffer B (5 μl), *lane 10*: 100 % of buffer B (5 μl).

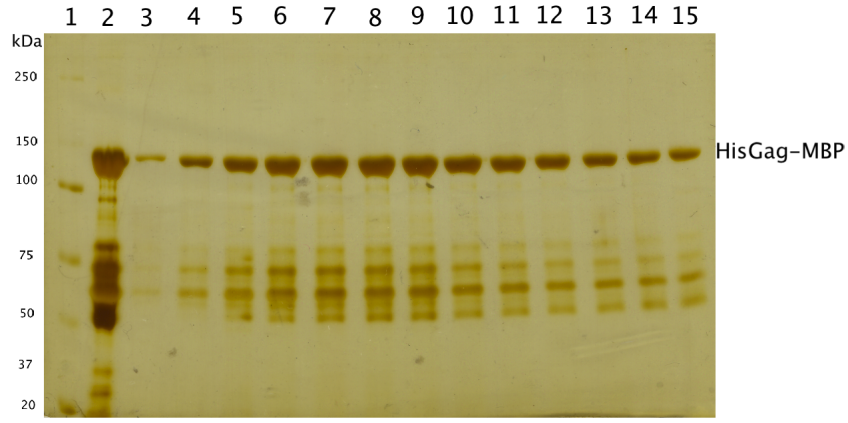

Figure 5.8: 10 % SDS PAGE gel showing purity of HisGag-MBP in elution fractions during gel permeation chromatography. *Lane 1*: MW standard (0.5 μl), *lane 2*: load (5 μl), *lanes 3-15*: protein fractions (10 μl).

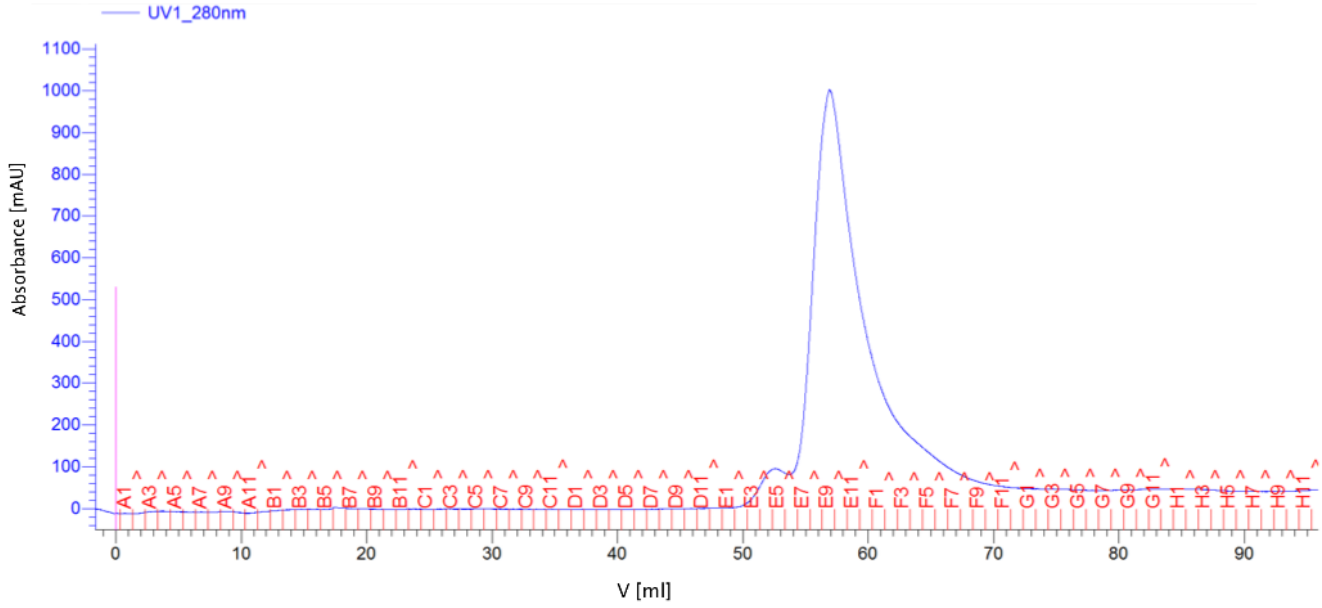

Figure 5.9: The chromatogram illustrating HisGag-MBP purification.

5.5 Determination of Kinetic Constants

The HisGag-MBP (in the solution of 20 mM Tris and 500 mM imidazole, pH = 8.0) was prepared as substrate for HIV-1 PR. The optimal conditions for HIV-1 PR activity is: 150 mM sodium acetate, 300 mM NaCl, 4 mM EDTA, pH 4.7. Therefore, the buffer (5 M sodium acetate, pH 4.4) was used to decrease pH in the final reaction mixture and the HisGag-MBP cleavage by HIV-1 PR was performed in the buffer with final pH 4.63 and 50 mM imidazole (chapter 4.5.1). The spectroscopic assay was performed to find out if the PR is active also in such conditions.

All the measurements were performed using the chromogenic peptide substrate KARVNIe↓NphEANIe-NH_2. The kinetic parameters for the wild-type and mutant proteinase (drv6) as well as the reference values in optimal conditions are summarized in **Table 5.1**. The Michaelis-Menten constant (K_m) and the turnover number (k_{cat}) are altered only slightly with respect to reference value. However, the efficiency of the substrate's cleavage of the wild-type PR (k_{cat}/K_m) decrease to the half and the efficiency of mutant PR remains almost the same.

Table 5.1: The kinetic parameters for the wild-type and the mutant drv6 HIV-1 PR [119].

	K_m (μM)	k_{cat} (s^{-1})	k_{cat}/K_m ($mM^{-1}s^{-1}$)
wild-type PR (optimal)	15 ± 1	30 ± 1.8	1990 ± 210
wild-type PR (final)	21 ± 0.7	20 ± 0.7	951.9 ± 12.9
mutant PR (optimal)	53 ± 2	9.6 ± 0.2	180 ± 7
mutant PR (final)	50.9 ± 5	8.9 ± 0.8	174.8 ± 2.8

5.6 Gag Processing by the Wild-type HIV-1 Proteinase

To determine the HisGag-MBP polyprotein processing by both wild-type and mutant HIV-1 PR, several reaction mixtures were prepared (chapter 4.5.2). The final volume of each reaction was 10 μl, in which the ratio of the substrate to enzyme was 20:1. All the cleavage reactions were performed at laboratory temperature and the process of cleavage was captured at different time points. Two controls were used, one without the addition of the PR (control 1) and one with the addition of the PR inhibitor darunavir (control 2). The samples were analyzed by SDS-PAGE and Western blotting.

The kinetics of HisGag-MBP by the wild-type proteinase is shown in **Figure 5.10**. The number of molecular mass of the bands were estimated according to expected molecular weight of the proteins. At the start of the experiment (0 h) and in both of the controls, the band of ∼97 kDa corresponding to the HisGag-MBP is clearly visible. After 1 h, the bands of ∼41 kDa and ∼56 kDa appear, that may correspond to the first products of PR cleavage MA-CA-p2 and NC-p1-p6-MBP. After 1 h, there are also visible bands of ∼48 kDa, ∼25 kDa, and ∼17 kDA, that may represent the structural proteins p6-MBP, CA and MA, respectively. The intensity of the bands is increasing in time (5 h, 10 h and 24 h). In the last lane, the CA marker is used, which represents the CA protein itself.

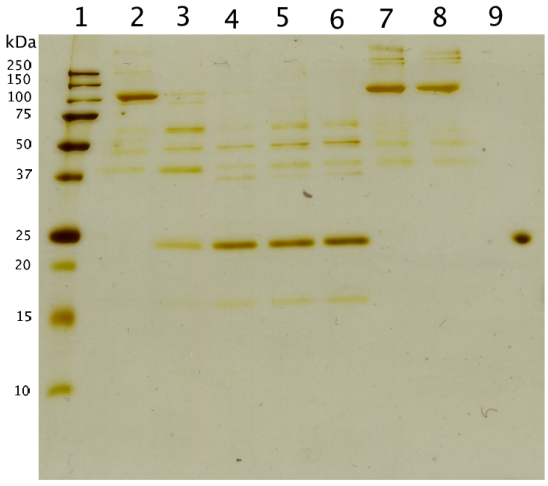

Figure 5.10: 18 % SDS PAGE gel showing processing of HisGag-MBP by the wild-type HIV-1 PR for different time periods *Lane 1*: MW standard (2 μl), *lane 2*: 0 h (14 μl), *lane 3*: 1 h (14 μl), *lane 4*: 5 h (14 μl), *lane 5*: 10 h (14 μl), *lane 6*: 24 h (14 μl), *lane 7*: control 1, 24 h (14 μl), *lane 8*: control 2, 24 h (14 μl), *lane 9*: CA marker (3 μl).

To clarify the cleavage products, Western blotting procedure using anti-capsid (**Figure 5.11a**) and anti-matrix antibodies (**Figure 5.11b**) was performed. The anti-capsid antibody recognizes the band of ∼97 kDa at 0 h and in both of the controls representing the HisGag-MBP. With increasing time, the bands of ∼41 kDa and ∼25 kDa appear, that correspond to the cleavage products CA-MA-p2 and CA. After 24 h, the band of ∼41 kDa is not visible.

The anti-matrix antibody visualizes the band of ∼97 kDa, ∼41 kDa and ∼18 kDa at the start of the experiment (0 h) and in both of the controls. These bands correspond to HisGag-MBP, CA-MA-p2 and the impurity with MA sequence. The band of ∼41 kDA decreases in time. After 1 h, the band of ∼17 kDa representing MA appears, and increase in time (5, 10 and 24 h).

Both the antibodies are specific mainly to free CA/MA and therefore the full-length HisGag-MBP protein is not very well visible on the blot.

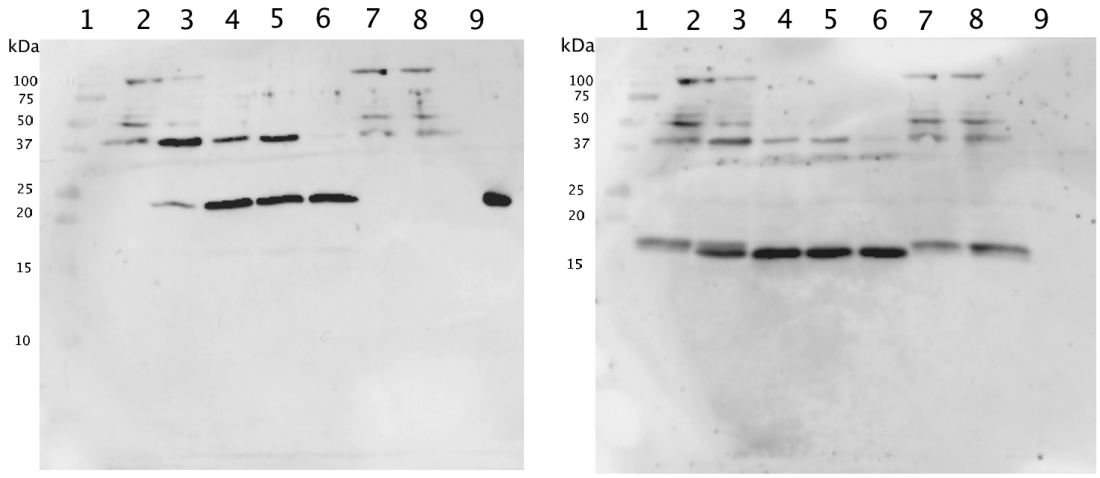

(a) (b)

Figure 5.11: Stripped Western blotting membrane showing processing of HisGag-MBP by the wild-type HIV-1 PR for different time periods (a) anti-capsid antibody (b) anti-matrix antibody *Lane 1*: MW standard (3 μl), *lane 2*: 0 h (14 μl), *lane 3*: 1 h (14 μl), *lane 4*: 5 h (14 μl), *lane 5*: 10 h (14 μl), *lane 6*: 24 h (14 μl), *lane 7*: control 1, 24 h (14 μl), *lane 8*: control 2, 24 h (14 μl), *lane 9*: CA marker (3 μl).

5.7 Gag Processing via Wild-type and Mutant HIV-1 Proteinase

To compare the Gag cleavage by the wild-type and mutant PRs, the same reactions as in chapter 5.6 were performed analysing also the drv6 HIV-1 PR [119] which is resistant to PI darunavir (**Figure 5.12**). At the start of the experiment (0 h) the band of ∼97 kDa is observed in reactions with wild-type and mutant PR, and in both of the controls. After 1 h, the bands of ∼56 kDa, ∼48 kDa and ∼41 kDa can be observed. The same bands appear also after 24 h in reaction with mutant HIV-1 PR and inhibitor darunavir (control 2). These bands correspond to the cleavage products NC-p1-p6-MBP, CA-MA-p2 and structural protein p6-MBP. After 5 h, in reactions with wild-type PR these bands disappear and the bands of ∼25 kDa and ∼17 kDa representing CA and MA can be seen. The amount of MA and CA increase over time (10 and 24 h). On the contrary, in reactions with mutant PR is visible the band of ∼41 kDa that decrease over time and the bands of ∼25 kDa and ∼17 kDa increase over time more slowly.

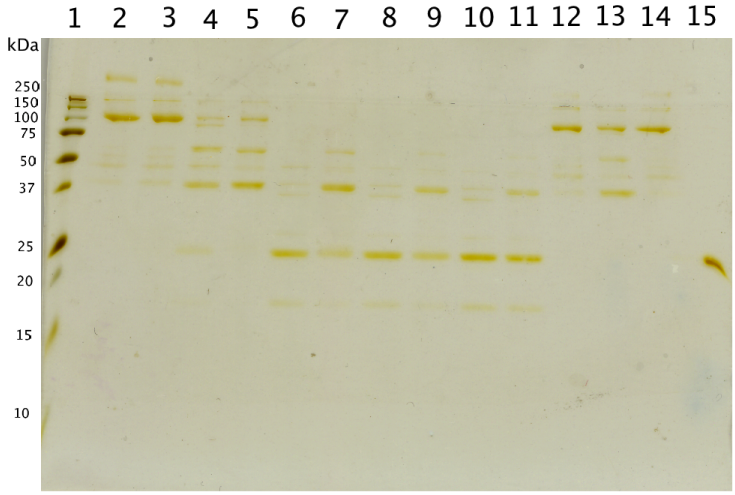

Figure 5.12: 18 % SDS PAGE gel showing processing of HisGag-MBP by the wild-type HIV-1 PR and drv6 for different time periods *Lane 1*: MW standard (2 μl), *lanes 2, 4, 6, 8, 10, 12*: wild-type PR, *lanes 3, 5, 7, 9, 11, 13*: drv6, *lanes 2,3*: 0 h (14 μl), *lanes 4,5*: 1 h (14 μl), *lanes 6,7*: 5 h (14 μl), *lanes 8,9*: 10 h (14 μl), *lanes 10,11*: 24 h (14 μl), *lanes 12,13*: control 2, 24 h (14 μl), *lane 14*: control 1, 24 h (14 μl), *lane 15*: CA marker (3 μl).

The products with CA (MA) sequence were recognized via anti-capsid (anti-matrix) antibody (**Figure 5.13**). The anti-capsid antibody visualized the band of ∼97 kDa after 0 h and in both of the controls corresponding to HisGag-MBP. The band of ∼41 kDa representing CA-MA-p2 appears after 1 h, and slowly disappears in reactions with wild-type PR. However, the band remains in reaction with mutant PR. This band can be seen also in control 2 with inhibitor darunavir and mutant PR. After 1 h, the band of ∼25 kDa representing CA is visible and slowly increases over time in reactions with wild-type PR. After 24 h, this band appears also in reactions with mutant PR.

On the stripped blot using anti-matrix antibody the same bands of ∼97 kDa and ∼41 kDa can be observed that represent HisGag-MBP and CA-MA-p2. Furthermore, the band of ∼18 kDa is visible at the start of the experiment, in both of the controls and in reaction using mutant PR. The band of ∼17 kDa corresponding to MA appears after 1 h of cleavage by the wild-type PR. After 5 h, the band can be seen also in reactions with mutant PR.

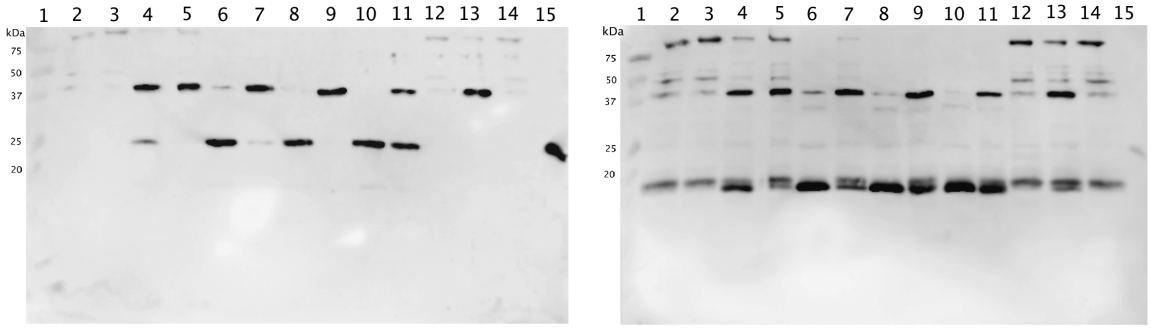

(a) (b)

Figure 5.13: Stripped Western blotting membrane showing processing of HisGag-MBP by the wild-type HIV-1 PR and drv6 for different time periods (a) anti-capsid antibody (b) anti-matrix antibody *Lane 1*: MW standard (3 μl), *lanes 2, 4, 6, 8, 10, 12*: wild-type PR, *lanes 3, 5, 7, 9, 11, 13*: drv6, *lanes 2,3*: 0 h (14 μl), *lanes 4,5*: 1 h (14 μl), *lanes 6,7*: 5 h (14 μl), *lanes 8,9*: 10 h (14 μl), *lanes 10,11*: 24 h (14 μl), *lanes 12,13*: control 2, 24 h (14 μl), *lane 14*: control 1, 24 h (14 μl), *lane 15*: CA marker (3 μl).

Chapter 6

Discussion

The regulation, order and rate of the Gag processing by HIV-1 proteinase has been investigated by several groups in order to design HIV-1 proteinase inhibitors.

In number of biochemical studies, short oligopeptides representing naturally occurring cleavage sites were used to obtain individual kinetic parameters [64, 69]. However, these data do not correspond with further work using full-length Gag polyprotein [71, 120]. In the work of Wondrak et al., 72 amino acid peptide containing one cleavage site was synthesized to avoid the employment of small peptides [121].

Peptide cleavage assays cannot reveal the relative rates of Gag processing, therefore the simulation of the native processing event was needed. This was done by cell-free expression system of full-length Gag polyprotein and the kinetic analysis clarified that Gag processing by HIV-1 proteinase was an ordered process [70, 71].

In this thesis, we propose to study Gag cleavage kinetics using the full-length substrate. Several studies of Gag polyprotein utilized the product with truncation in the N-terminal MA domain or C-terminal p6 domain in order to disrupt the Gag aggregation [122, 123]. Carlson et al. described the expression of the full-length Gag polyprotein [124] using heparin column in addition to other conventional techniques. In our study, we prepared three His- and MBP-tagged full-length Gag polyprotein variants (Gag-MBP, HisGag-MBP, Gag-MBPHis). The MBP tag provides protection of C-terminal p6 domain and it allows us to separate the target protein from its degradation products, which result from the

Gag cleavage within the p6 region by bacterial proteinases during the expression and purification process. Furthermore, MBP improves the solubility of the protein and can be used for purification on amylose column, although it was finally not used in this work. In the kinetic assay, where the sequence and rate of individual cleavages is studied, the fusion protein allows us to observe also the C-terminal cleavage products by SDS-PAGE, which are otherwise short and hardly visible.

All three constructs were cloned and expressed in *E.coli*. HisGag-MBP variant was purified and used in kinetic experiments with the wild-type HIV-1 proteinase. Because Gag precipitates in imidazole-free buffer, 50 mM imidazole in each cleavage reaction was present to stabilize the substrate. The originally basic pH was adjusted to 4.4 by the addition of acidic acetate buffer in order to reach the optimum conditions for PR cleavage. The PR activity was verified by spectroscopic assay using chromogenic peptide substrate.

We analyzed the cleavage products by SDS-PAGE and Western blotting using antibodies against capsid and matrix proteins. We are able to observe the p2↓NC cleavage by the wild-type PR. The products are visible after 1 h, and than they are cleaved to final structural proteins. The cleavage at MA↓CA and p2↓NC is visible on the gel and blot as the gradual increase of MA and CA proteins over time. The other cleavages are difficult to be observed by these methods. The p1↓p6 cleavage can be seen on the gels, but the products are not well stainable, therefore it is not possible to evaluate the kinetics. The NC↓p1 cleavage cannot be observed at all, as the products are small and invisible on the gel. Both these processes would be better observable with the eventual use of anti-nucleocapsid antibody, which was currently inaccessible to us. The most questionable point is the CA↓p2 cleavage. As the detection of the proteins by the anti-capsid antibody is highly sensitive, a double band of 2 kDa difference of bands can be expected as a consequence of this cleavage. However, only a single band is observed on all the gels and blots. This can be explained either by a small mobility difference of the two proteins or, as the observed bands correspond well with the CA standard, by very high rate of the PR cleavage. However, rates of this cleavage are generally slow [71], therefore the latter option seems less likely. This question can be resolved by the method of mass spectrometry.

Furthermore, the cleavage experiments within this diploma thesis are carried out with the purified HisGag-MBP that contains a minor degradation product that has not been completely removed in the purification process. The product can be seen in the non-processed Gag at 0 h and in all the control reactions. As it is detected only by the anti-matrix antibody and its molecular weight is slightly higher than that of MA, it seems to be MA protein extended by a short part of CA. This idea is confirmed also by the fact that the band of this protein vanishes during the proteolytic cleavage by HIV-1 PR and changes most likely to the MA and a short peptide invisible on the blot. However, the total amount of this degradation product is likely very low because it is not visible on SDS-PAGE gel, but only on the very sensitive blot with anti-matrix antibody. Nevertheless, the presence of this band does not complicate the interpretation of the kinetic experiments remarkably.

We observe also the influence of the mutations in proteinase on the rate and order of Gag processing. We have chosen drv6 HIV-1 PR [119], that has the twenty-one mutations and thus its activity varies from that of the wild-type HIV-1 PR. The simultaneously carried out reactions with both wild-type and mutant PR show, that the mutated PR processes Gag with decreased rate, but the decrease is not equal for all the cleavage sites. The first cleavage between the p2 and NC peptides runs in both cases with relatively high velocity. Full-length Gag is almost completely processed after 1 h, although in the case of the mutant proteinase the process seems to be somewhat slower. The most significant difference can be observed at the second cleavage between MA and CA proteins. Although the cleavage by wild-type PR is observable already after 1 h and is almost complete after 5 h, cleavage by the mutant variant of PR is barely visible after 5 and 10 h and a substantial portion of MA-CA-p2 substrate is processed only after 24 h. Thus, this cleavage site is probably more sensitive to the structural changes induced by individual mutations than the p2↓NC site. This indicates that this cleavage can make the considerable difference in the life-cycle periods of the wild-type and mutated virus. Hence, it is conceivable that the purpose of the subsequent mutations in the Gag cleavage sites is to compensate the rate decrease rather than to force the inhibitor out of the active-site cavity of PR [111, 112].

The reason is that the enzyme-inhibitor affinity is so high that a structural rearrangement of the substrate would have to be improbably efficient in order to influence this equilibrium considerably. However, this assumption has to be confirmed by additional experiments with the mutated Gag polyprotein. These experiments were originally planned for this thesis, but they had to be postponed, because the clone of the mutated Gag has not been delivered to us by the collaborating foreign laboratory in time.

This experiment represents the background to assess the dependence of cleavage rates for individual mutations in HIV-1 proteinase. We plan to carry out the experiments with more mutant variants of HIV-1 PR that are present in our laboratory. Furthermore, the role of mutations in Gag polyprotein should be studied, therefore a production of several Gag variants will be necessary, which will be used in the kinetic assays with the wild-type and mutant HIV-1 PR. This should provide a better insight into the process of mutagenesis of HIV virus under the selection pressure of inhibitors and help us to elucidate the causative relations among the development of mutation in different viral proteins and their specific sites.

Although the presented study describes a way how to determine the cleavage kinetics of Gag processing by PR, a reliable quantitative statement cannot be obtained from it. Therefore, further analysis by more sophisticated methods are planned for the future continuation of these experiments. The method of capillary electrophoresis in the regime of capillary gel electrophoresis represents a suitable choice. Here, the capillary is filled by polyacrylamide solution and the separation is performed in the presence of SDS, therefore the method is a direct analogy of SDS-PAGE, which enables us an easy interpretation. Another alternative is LC/MS, i.e. the HPLC separation of cleavage products followed by both UV and MS detection. The advantage of this technique is the unambiguous detection of the products, but, on the contrary, the optimization of this method for simultaneous separation of all the products can be a more complex problem. Both the methods have already been applied to our samples, but reproducible results have not been obtained from either of them yet due to the lack of time. Therefore, these experiments are not reported in this thesis, but they are planned to be carried out in the future.

Conclusion

To study the Gag processing by HIV-1 proteinase, the recombinant full-length Gag polyprotein that represents the natural substrate is needed. For this purpose, three C-terminally MBP-tagged Gag variants (Gag-MBP, HisGag-MBP and Gag-MBPHis) were cloned into expression vector pET22b and recombinantly expressed in *E.coli* BL21(DE3)RIL. HisGag-MBP was purified with the yield of 1 mg/l of bacterial culture. HisGag-MBP was cleaved by both the wild-type and mutant HIV-1 proteinase and the cleavage products were analyzed via SDS-PAGE and Western blotting. Substantial decrease have been observed for the cleavage rate of Gag by wild-type HIV-1 PR in comparison with the mutant variant, especially for the MA↓CA site. This indicates that the subsequently developed mutations in the cleavage sites may serve the virus to compensate this rate decrease.

Although not all originally defined goals have been achieved, this diploma thesis represents a background to study Gag processing in more detail using a natural substrate. For future experiments, the optimization of Gag purification will be needed to obtain pure and stable protein. The products of Gag cleavage by PR will be analyzed by quantitative methods like LC/MS or capillary electrophoresis. In order to complete the study, it is planned to analyze the influence of mutations in Gag polyprotein on PR cleavage and thus to evaluate their effect on HIV resistance.

References

[1] J.C. Chermann, F. Rey, M.T. Nugeyre, S. Chamaret, J. Gruest, C. Dauguet, C. Rouzioux, W. Rozenbaum, and L. Montagnier. Isolation of a T-Lymphotropic Retrovirus from a Patient at Risk for Acquired Immune Deficiency Syndrome (AIDS). *Science*, 220(4599):868–871, 1983.

[2] R.C. Gallo. The AIDS Virus. *Sci Am*, 256(1):46–56, 1987.

[3] S. Colombini, S.K. Arya, M.S. Reitz, L. Jagodzinski, B. Beaver, and F. Wong-Staal. Structure of simian immunodeficiency virus regulatory genes. *P Natl Acad Sci USA*, 86(13):4813–4817, 1989.

[4] P.B. Gilbert, I.W. McKeague, G. Eisen, C. Mullins, A. Guéye-NDiaye, S. Mboup, and P.J. Kanki. Comparison of HIV-1 and HIV-2 infectivity from a prospective cohort study in Senegal. *Stat Med*, 22(4):573–593, 2003.

[5] F. Gao, L. Yue, D.L. Robertson, S.C. Hill, H. Hui, R.J. Biggar, P.M. Sharp, and B.H. Hahn. Genetic diversity of human immunodeficiency virus type 2 : evidence for distinct sequence subtypes with differences in virus biology. *J Virol*, 68(11): 7433–7447, 1994.

[6] M.S. Gottlieb, R. Schroff, H.M. Schanker, J.D. Weisman, P.T. Fan, R.A. Wolf, and A. Saxon. Pneumocystis carinii pneumonia and mucosal candidiasis in previously healthy homosexual men: evidence of a new acquired cellular immunodeficiency. *N Engl J Med*, 305(24):1425–1431, 1981.

[7] Global Health Observatory Data Repository, Acquired on, March 2013. URL http://apps.who.int/gho/data/?vid=22100.

[8] A.S. Perelson, A.U. Neumann, M. Markowitz, J.M. Leonard, and D.D. Ho. HIV-1 Dynamics in Vivo: Virion Clearance Rate, Infected Cell Life-Span, and Viral Generation Time. *Science*, 271:1582–1586, 1996.

[9] M. Gouwy, S. Struyf, N. Berghmans, C. Vanormelingen, D. Schols, and J. van Damme. CXCR4 and CCR5 ligands cooperate in monocyte and lymphocyte migration and in inhibition of dual-tropic (R5/X4) HIV-1 infection. *Eur J Immunol*, 41(4):963–973, 2011.

[10] R.W. Doms and S.C. Peiper. Unwelcomed Guests with Master Keys: How HIV Uses Chemokine Receptors for Cellular Entry. *Virology*, 190(235):179–190, 1997.

[11] E.O. Freed. HIV-1 Gag Proteins : Diverse Functions in the Virus Life Cycle. *Virology*, 15(251):1–15, 1998.

[12] B. Ganser-Pornillos, M. Yeager, and W.I. Sundquist. The structural biology of HIV assembly. *Curr Opin Struct Biol*, 18(2):203–217, 2008.

[13] E.O. Freed. HIV-1 replication. *Somat Cell Molec Gen*, 26(1-6):13–33, 2001.

[14] C.L. Woodward and S.A. Chow. A new dynamic in HIV-1 replication. *Nucleus*, 1 (1):18–22, 2010.

[15] D.G. Demirov and E.O. Freed. Retrovirus budding. *Virus Res*, 106(2):87–102, 2004.

[16] E. Morita and W.I. Sundquist. Retrovirus budding. *Annu Rev Cell Dev Bi*, 20: 395–425, 2004.

[17] T. Jacks, M.D. Power, F.R. Masiarz, P.A. Luciw, P.J. Barr, and H.E. Varmus. Characterization of ribosomal frameshifting in HIV-1 gag-pol expression. *Nature*, 331(6153):280–283, 1988.

[18] B. Ganser-Pornillos, M. Yeager, and W.I. Sundquist. The Structural Biology of HIV Assembly. *Curr Opin Struct Biol*, 18(2):1–24, 2010.

[19] J.W. Wills and R.C. Craven. Form, function, and use of retroviral Gag proteins. *AIDS*, 5:639–654, 1991.

[20] G. Mirambeau, S. Lyonnais, and R.J. Gorelick. Features, processing states, and heterologous protein interactions in the modulation of the retroviral nucleocapsid protein function. *RNA Biol*, 7(6):724–734, 2010.

[21] M.A. Massiah, M.R. Starich, C. Paschall, M.F. Summers, A.M. Christensen, and W.I. Sundquist. Three-Dimensional Structure of the Human Immunodeficiency Virus Type 1 Matrix Protein. *J Mol Biol*, 244(2):198–223, 1994.

[22] M. Facke, A. Janetzko, and R.L. Shoeman. A large deletion in the matrix domain of the human immunodeficiency virus gag gene redirects virus particle assembly from the plasma membrane to the endoplasmic. *J Virol*, 67(8):4972–4980, 1993.

[23] M. Huang and M.A. Martin. Incorporation of Pr160 (gag-pol) into virus particles requires the presence of both the major homology region and adjacent C-terminal capsid sequences within the Gag-Pol. *J Virol*, 71(6):4472–4478, 1997.

[24] A. Ono, H. Mingjun, and E.O. Freed. Characterization of human immunodeficiency virus type 1 matrix revertants : effects on virus assembly , Gag processing , and Env incorporation into virions. *J Virol*, 71(6):4409–4418, 1997.

[25] T.R. Gamble, S. Yoo, F.F. Vajdos, U.K. von Schwedler, D.K. Worthylake, H. Wang, J.P. McCutcheon, W.I. Sundquist, and C.P. Hill. Structure of the carboxyl-terminal dimerization domain of the HIV-1 capsid protein. *Science*, 278:849–853, 1997.

[26] B. Kattenbeck, A. von Poblotzki, A. Rohrhofer, H. Wolf, and S. Modrow. Inhibition of human immunodeficiency virus type 1 particle formation by alterations of defined amino acids within the C terminus of the capsid protein. *J Gen Virol*, 78:2489–2496, 1997.

[27] C. Tang, Y. Ndassa, and M.F. Summers. Structure of the N-terminal 283-residue fragment of the immature HIV-1 Gag polyprotein. *Nat Struct Biol*, 9(7):537–543, 2002.

[28] M. Grättinger, H. Hohenberg, D. Thomas, T. Wilk, B. Müller, and H.-G. Kraüsslich. In vitro assembly properties of wild-type and cyclophilin-binding defective human immunodeficiency virus capsid proteins in the presence and absence of cyclophilin A. *Virology*, 257(1):247–260, 1999.

[29] T.L. South and M.F. Summers. Zinc- and sequence-dependent binding to nucleic acids by the N-terminal zinc finger of the HIV-1 nucleocapsid protein: NMR structure of the complex with the Psi-site analog, dACGCC. *Protein Sci*, 2(1):3–19, 1993.

[30] C. Meric, J.-L. Darlix, and P.-F. Spahr. It is Rous Sarcoma virus protein P12 and not P19 that binds tightly to Rous Sarcoma virus RNA. *J Mol Biol*, 173(4):531–538, 1984.

[31] H.G. Göttlinger, T. Dorfman, J.G. Sodroski, and W.A. Haseltine. Effect of mutations affecting the p6 gag protein on human immunodeficiency virus particle release. *P Natl Acad Sci USA*, 88(8):3195–3199, 1991.

[32] M. Huang, J.M. Orenstein, M.A. Martin, and E.O. Freed. p6Gag is required for particle production from full-length human immunodeficiency virus type 1 molecular clones expressing protease. *J Virol*, 69(11):6810–6818, 1995.

[33] E.R. Wright, J.B. Schooler, H.J. Ding, C. Kieffer, C. Fillmore, W.I. Sundquist, and G.J. Jensen. Electron cryotomography of immature HIV-1 virions reveals the structure of the CA and SP1 Gag shells. *EMBO J*, 26(8):2218–2226, 2007.

[34] S. Datta, L.G. Temeselew, R.M. Crist, F. Soheilian, A. Kamata, J. Mirro, D. Harvin, K. Nagashima, R.E. Cachau, and A. Rein. On the role of the SP1 domain in HIV-1 particle assembly: a molecular switch? *J Virol*, 85(9):4111–4121, 2011.

[35] A. De Marco, A.M. Heuser, B. Glass, H.-G. Kraüsslich, B. Müller, and J.A.G. Briggs. The role of the SP2 domain and its proteolytic cleavage in HIV-1 structural maturation and infectivity. *J Virol*, 86(26):13708–13716, 2012.

[36] S.G. Sarafianos, B. Marchand, K. Das, D. Himmel, A. Michael, S.H. Hughes, and E. Arnold. Structure and function of HIV-1 reverse transcriptase: molecular mechanisms of polymerization and inhibition. *J Mol Biol*, 385(3):693–713, 2010.

[37] A. Telesnitsky and S.P. Goff. Reverse Transcriptase and the Generation of Retroviral DNA. In JM Coffin, SH Hughes, and HE Varmus, editors, *Retroviruses*, pages 121–160. Cold Spring Harbor (NY): Cold Spring Harbor Laboratory Press, 1997.

[38] H. Chen, S.Q. Wei, and A. Engelman. Multiple integrase functions are required to form the native structure of the human immunodeficiency virus type I intasome. *J Biol Chem*, 274(24):17358–17364, 1999.

[39] P.O. Brown. Integration. In JM Coffin, SH Hughes, and HE Varmus, editors, *Retroviruses*. Cold Spring Harbor (NY): Cold Spring Harbor Laboratory Press, 1997.

[40] A. Leiherer, C. Ludwig, and R. Wagner. Uncoupling human immunodeficiency virus type 1 Gag and Pol reading frames: role of the transframe protein p6* in viral replication. *J Virol*, 83(14):7210–7220, 2009.

[41] M. Moulard and E. Decroly. Maturation of HIV envelope glycoprotein precursors by cellular endoproteases. *Biochim Biophys Acta*, 1469(3):121–132, 2000.

[42] C.K. Leonard, M.W. Spellman, L. Riddle, R.J. Harris, J.N. Thomas, and T.J. Gregory. Assignment of intrachain disulfide bonds and characterization of potential glycosylation sites of the type 1 recombinant human immunodeficiency virus envelope glycoprotein (gp120) expressed in Chinese hamster ovary cells. *J Biol Chem*, 265(18):10373–10382, 1990.

[43] P.D. Kwong, R. Wyatt, J. Robinson, R.W. Sweet, J. Sodroski, and W.A. Hendrick-

son. Structure of an HIV gp120 envelope glycoprotein in complex with the CD4 receptor and a neutralizing human antibody. *Nature*, 393(6686):648–659, 1998.

[44] A.D. Frankel and J.A.T. Young. HIV-1: fifteen proteins and an RNA. *Annu Rev Biochem*, 67:1–25, 1998.

[45] M.G. Mateu. The capsid protein of human immunodeficiency virus: intersubunit interactions during virus assembly. *Febs J*, 276(21):6098–6109, 2009.

[46] S.D. Fuller, T. Wilk, B.E. Gowen, H.-G. Kraüsslich, and V.M. Vogt. Cryo-electron microscopy reveals ordered domains in the immature HIV-1 particle. *Curr Biol*, 7 (10):729–738, 1997.

[47] E.B. Monroe, S. Kang, S.K. Kyere, R. Li, and P.E. Prevelige. Hydrogen/deuterium exchange analysis of HIV-1 capsid assembly and maturation. *Structure*, 18(11): 1483–1491, 2010.

[48] M. Bryant and L. Ratner. Myristoylation-dependent replication and assembly of human immunodeficiency virus 1. *P Natl Acad Sci USA*, 87(2):523–527, 1990.

[49] C. Tang, J.M. Louis, A. Aniana, J.-Y. Suh, and G.M. Clore. Visualizing transient events in amino-terminal autoprocessing of HIV-1 protease. *Nature*, 455(7213):693–696, 2008.

[50] A. De Marco, B. Müller, B. Glass, J.D. Riches, H.-G. Kraüsslich, and J.A.G. Briggs. Structural analysis of HIV-1 maturation using cryo-electron tomography. *PLoS Pathog*, 6(11):e1001215, 2010.

[51] E. De Clercq. Anti-HIV drugs: 25 compounds approved within 25 years after the discovery of HIV. *Int J Antimicrob Ag*, 33(4):307–320, 2009.

[52] U.S. Food and Drug Administration. Acquired on, March 2013. URL `http://www.fda.gov/ForConsumers/ByAudience/ForPatientAdvocates/ /HIVandAIDSActivities/ucm118915.htm`.

[53] E.A. Berger, P.M. Murphy, and J.M. Farber. Chemokine receptors as HIV-1 coreceptors: roles in viral entry, tropism, and disease. *Annu Rev Immunol*, 17:657–700, 1999.

[54] E. De Clercq. Non-nucleoside reverse transcriptase inhibitors (NNRTIs): past, present, and future. *Chem Biodivers*, 1(1):44–64, 2004.

[55] D.A. Cooper, R.T. Steigbigel, J.M. Gatell, J.K. Rockstroh, C. Katlama, P. Yeni, A. Lazzarin, B. Clotet, P.N. Kumar, J.E. Eron, M. Schechter, M. Markowitz, M.R. Loutfy, J.L. Lennox, J. Zhao, J. Chen, D.M. Ryan, R.R. Rhodes, J.A. Killar, L.R. Gilde, K.M. Strohmaier, A.R. Meibohm, M.D. Miller, D.J. Hazuda, M.L. Nessly, M.J. DiNubile, R.D. Isaacs, H. Teppler, and B.-Y. Nguyen. Subgroup and resistance analyses of raltegravir for resistant HIV-1 infection. *N Engl J Med*, 359(4):355–365, 2008.

[56] J. Pokorná, L. Machala, P. Rezáčová, and J. Konvalinka. Current and Novel Inhibitors of HIV Protease. *Viruses*, 1(3):1209–1239, 2009.

[57] M.A. Navia, P. Fitzgerald, B.M. McKeever, C.-T. Leu, J.C. Heimbach, W.K. Herber, I.S. Sigal, P.L. Darke, and J.P. Springer. Three-dimensional structure of aspartyl protease from human immunodeficiency virus HIV-1. *Nature*, 337(6208):615–620, 1989.

[58] M. Miller, M. Jaskolski, K.M. Rao, J. Leis, and A. Wlodawer. Crystal structure of a retroviral protease proves relationship to aspartic protease family. *Nature*, 337 (6207):576–579, 1989.

[59] D.M. York, T.A. Darden, L.G. Pedersen, and M.W. Anderson. Molecular Modeling Studies Suggest That Zinc Ions Inhibit HIV-1 Protease by Binding at Catalytic Aspartates. *Environ Health Persp*, 101(3):246–250, 2013.

[60] A. Wlodawer and J. Vondrasek. Inhibitors of HIV-1 protease: a major success of structure-assisted drug design. *Annu Rev Bioph Biom*, 27:249–284, 1998.

[61] R. Ishima, D.I. Freedberg, Y.-X. Wang, J.M. Louis, and D. Torchia. Flap opening and dimer-interface flexibility in the free and inhibitor-bound HIV protease, and their implications for function. *Structure*, 7(9):1047–1055, 1999.

[62] V. Hornak, A. Okur, R.C. Rizzo, and C. Simmerling. HIV-1 protease flaps spontaneously open and reclose in molecular dynamics simulations. *P Natl Acad Sci USA*, 103(4):915–920, 2006.

[63] J. Tözsér. Comparative studies on retroviral proteases: substrate specificity. *Viruses*, 2(1):147–165, 2010.

[64] J. Tözsér, I. Bláha, T.D. Copeland, E.M. Wondrak, and S. Oroszlan. Comparison of the HIV-1 and HIV-2 proteinases using oligopeptide substrates representing cleavage sites in Gag and Gag-Pol polyproteins. *Febs Lett*, 281(1-2):77–80, 1991.

[65] J.T. Griffiths, L.H. Phylip, J. Konvalinka, P. Strop, A. Gustchina, A. Wlodawer, R.J. Davenport, R. Briggs, B.M. Dunn, and J. Kay. Different requirements for productive interaction between the active site of HIV-1 proteinase and substrates containing -hydrophobic-hydrophobic- or -aromatic-Pro- cleavage sites. *Biochemistry*, 31(22): 5193–5200, 1992.

[66] J. Tözsér, I.T. Weber, A. Gustchina, I. Bláha, T.D. Copeland, J.M. Louis, and S. Oroszlan. Kinetic and Modeling Studies of S3-S3/ Subsites of HIV Proteinases. *Biochemistry*, (1987):4793–4800, 1992.

[67] M. Prabu-Jeyabalan, E.A. Nalivaika, and C.A. Schiffer. Substrate shape determines specificity of recognition for HIV-1 protease: analysis of crystal structures of six substrate complexes. *Structure*, 10(3):369–381, 2002.

[68] I.T. Weber and J. Agniswamy. HIV-1 Protease: Structural Perspectives on Drug Resistance. *Viruses*, 1(3):1110–1136, 2009.

[69] A. Fehér, I.T. Weber, P. Bagossi, P. Boross, B. Mahalingam, J.M. Louis, T.D. Copeland, I.Y. Torshin, R.W. Harrison, and J. Tözsér. Effect of sequence polymorphism

and drug resistance on two HIV-1 Gag processing sites. *Eur J Biochem*, 269(16): 4114–4120, 2002.

[70] S.C. Pettit, G.J. Henderson, C.A. Schiffer, and R. Swanstrom. Replacement of the P1 Amino Acid of Human Immunodeficiency Virus Type 1 Gag Processing Sites Can Inhibit or Enhance the Rate of Cleavage by the Viral Protease. *J Virol*, 76(20): 10226–10233, 2002.

[71] S.C. Pettit, M.D. Moody, R.S. Wehbie, A.H. Kaplan, P.V. Nantermet, C.A. Klein, and R. Swanstrom. The p2 domain of human immunodeficiency virus type 1 Gag regulates sequential proteolytic processing and is required to produce fully infectious virions. *J Virol*, 68(12):8017–8027, 1994.

[72] P.D. Yin, D. Das, and H. Mitsuya. Overcoming HIV drug resistance through rational drug design based on molecular, biochemical, and structural profiles of HIV resistance. *Cell Mol Life Sci*, 63(15):1706–1724, 2006.

[73] P.M. Colman. New antivirals and drug resistance. *Annu Rev Biochem*, 78:95–118, 2009.

[74] N.A. Roberts, J.A. Martin, D. Kinchington, A.V. Broadhurst, C. Craig, I.B. Duncan, S.A. Galpin, B.K. Handa, J. Kay, A. Kröhn, R.W. Lambert, J.H. Merrett, J.S. Mills, K.E. Parkes, S. Redshaw, A.J. Ritchie, D.L. Taylor, G.J. Thomas, and P.J. Machin. Rational Design of Peptide-Based HIV Proteinase. *Science*, 248:358–361, 1990.

[75] A. Wlodawer. Rational approach to AIDS drug design through structural biology. *Annu Rev Med*, 53(6):595–614, 2002.

[76] D.J. Kempf, K.C. Marsh, L.C. Fino, P. Bryant, A. Craig-Kennard, H.L. Sham, C. Zhao, S. Vasavanonda, W.E. Kohlbrenner, N.E. Wideburg, A. Saldivar, B.E. Green, T. Herrin, and D. Norbeck. Design of orally bioavailable, symmetry-based inhibitors of HIV protease. *Bioorgan Med Chem*, 2(9):847–858, 1994.

[77] G.N. Kumar, A.D. Rodrigues, A.M. Buko, and J.F. Denissen. Cytochrome P450-mediated metabolism of the HIV-1 protease inhibitor ritonavir (ABT-538) in human liver microsomes. *J Pharmacol Exp Ther*, 277(1):423–431, 1996.

[78] B.D. Dorsey, R.B. Levin, S.L. McDaniel, J.P. Vacca, J.P. Guare, P.L. Darke, J.A. Zugay, E.A. Emini, and W.A. Schleif. L-735,524: the design of a potent and orally bioavailable HIV protease inhibitor. *J Med Chem*, 37(21):3443–3451, 1994.

[79] A.K. Patick, H. Mo, M. Markowitz, K. Appelt, B. Wu, L. Musick, S. Kaldor, S. Reich, D.D. Ho, and S. Webber. Antiviral and resistance studies of AG1343 , an orally bioavailable inhibitor of human immunodeficiency virus protease. *Antimicrob Agents Ch*, 40(2):292–297, 1996.

[80] E.E. Kim, C.T. Baker, M.D. Dwyer, M.A. Murcko, B.G. Rao, R.D. Tung, and M.A. Navia. Crystal structure of HIV-1 protease in complex with VX-478, a potent and orally bioavailable inhibitor of the enzyme. *J Am Chem Soc*, 117(3):1181–1182, 1995.

[81] P. Vierling and J. Greiner. Prodrugs of HIV protease inhibitors. *Curr Pharm Design*, 9(22):1755–1770, 2003.

[82] E. De Clercq. New developments in anti-HIV chemotherapy. *Biochim Biophys Acta*, 1587(2-3):258–275, 2002.

[83] S.M. Poppe, D.E. Slade, K.-T. Chong, R.R. Hinshaw, P.J. Pagano, M. Markowitz, D.D. Ho, H. Mo, R.R. Gorman, T.J. Dueweke, S. Thaisrivongs, and W.G. Tarpley. Antiviral activity of the dihydropyrone PNU-140690 , a new nonpeptidic human immunodeficiency virus protease inhibitor. *Antimicrob Agents Ch*, 41(5):1058–1063, 1997.

[84] N. Merchante, L.F. López-Cortés, M. Delgado-Fernández, M.J. Ríos-Villegas, M. Márquez-Solero, D. Merino, J. Pasquau, C. García-Figueras, M.A. Martínez-Pérez, M. Omar, A. Rivero, J. Macías, R. Mata, and J.A. Pineda. Liver toxicity of antiretroviral combinations including fosamprenavir plus ritonavir 1400/100 mg

once daily in HIV/hepatitis C virus-coinfected patients. *AIDS Patient Care ST*, 25 (7):395–402, 2011.

[85] Y. Koh, H. Nakata, K. Maeda, G. Bilcer, T. Devasamudram, J.F. Kincaid, P. Boross, Y.-F. Wang, Y. Tie, P. Volarath, L. Gaddis, R.W. Harrison, T. Weber, A.K. Ghosh, H. Mitsuya, H. Ogata, and I.T. Weber. Novel bis Nonpeptidic Protease Inhibitor (PI) UIC-94017 (TMC114) with Potent Activity against Multi-PI-Resistant Human Immunodeficiency Virus In Vitro. *Antimicrob Agents Ch*, 47(10):3123–3129, 2003.

[86] C.S. Adamson and E.O. Freed. Novel Approaches to Inhibiting HIV-1 Replication. *Antivir Res*, 85(1):1–55, 2011.

[87] A.H. Kaplan, J. Zack, M. Knigge, D. Paul, D.J. Kempf, D. Norbeck, and R. Swanstrom. Partial inhibition of the human immunodeficiency virus type 1 protease results in aberrant virus assembly and the formation of noninfectious particles. *J Virol*, 67(7):4050–4055, 1993.

[88] C.S. Adamson, K. Salzwedel, and E.O. Freed. Virus Maturation as a Novel HIV-1 Therapeutic Target. *Expert Opin Ther Tar*, 13(8):895–908, 2009.

[89] T. Fujioka, Y. Kashiwada, R.E. Kilkuskie, L.M. Cosentino, L.M. Ballas, J.B. Jiang, W.P. Janzen, I.-S. Chen, and K.-H. Lee. Anti-AIDS Agents, 11. Betulinic Acid and Platanic Acid as Anti-HIV Principles from Syzigium claviflorum, and the Anti-HIV Activity of Structurally Related Triterpenoids. *J Nat Prod*, 57(2):243–247, 1994.

[90] Y. Kashiwada, F. Hashimoto, L.M. Cosentino, C.H. Chen, P.E. Garrett, and K.-H. Lee. Betulinic Acid and Dihydrobetulinic Acid Derivatives as Potent Anti-HIV Agents1. *J Med Chem*, 39(5):1016–1017, 1996.

[91] C. Tang, E. Loeliger, I. Kinde, S.K. Kyere, K. Mayo, E. Barklis, Y. Sun, M. Huang, and M.F. Summers. Antiviral Inhibition of the HIV-1 Capsid Protein. *J Mol Biol*, 327(5):1013–1020, 2003.

[92] J. Zhou, L. Huang, D.L. Hachey, C.H. Chen, and C. Aiken. Inhibition of HIV-1 maturation via drug association with the viral Gag protein in immature HIV-1 particles. *J Biol Chem*, 280(51):42149–42155, 2005.

[93] D.E. Martin, K. Salzwedel, and G.P. Allaway. Review Bevirimat : a novel maturation inhibitor for the treatment of HIV-1 infection. *Adv Exp Med Biol*, 19:107–113, 2008.

[94] A.T. Nguyen, C.L. Feasley, K.W. Jackson, T.J. Nitz, K. Salzwedel, G.M. Air, and M. Sakalian. The prototype HIV-1 maturation inhibitor, bevirimat, binds to the CA-SP1 cleavage site in immature Gag particles. *Retrovirology*, 8(1):101–114, 2011.

[95] F. Li, D. Zoumplis, C. Matallana, N.R. Kilgore, M. Reddick, A.S. Yunus, C.S. Adamson, K. Salzwedel, D.E. Martin, G.P. Allaway, E.O. Freed, and C.T. Wild. Determinants of activity of the HIV-1 maturation inhibitor PA-457. *Virology*, 356 (1-2):217–224, 2006.

[96] P.W. Keller, C.S. Adamson, J.B. Heymann, E.O. Freed, and A.C. Steven. HIV-1 maturation inhibitor bevirimat stabilizes the immature Gag lattice. *J Virol*, 85(4): 1420–1428, 2011.

[97] F. Li, R. Goila-Gaur, K. Salzwedel, N.R. Kilgore, M. Reddick, C. Matallana, A. Castillo, D. Zoumplis, D.E. Martin, J.M. Orenstein, G.P. Allaway, E.O. Freed, and C.T. Wild. PA-457: a potent HIV inhibitor that disrupts core condensation by targeting a late step in Gag processing. *P Natl Acad Sci USA*, 100(23):13555–13560, 2003.

[98] K. Salzwedel, D.E. Martin, and M. Sakalian. Maturation Inhibitors: a New Therapeutic Class Targets the Virus Structure. *AIDS Rev*, (9):162–172, 2007.

[99] C.S. Adamson, K. Waki, S.D. Ablan, K. Salzwedel, and E.O. Freed. Impact of human immunodeficiency virus type 1 resistance to protease inhibitors on evolution of resistance to the maturation inhibitor bevirimat (PA-457). *J Virol*, 83(10):4884–4894, 2009.

[100] J. Zhou, C.H. Chen, and C. Aiken. The sequence of the CA-SP1 junction accounts for the differential sensitivity of HIV-1 and SIV to the small molecule maturation inhibitor 3-O-{3',3'-dimethylsuccinyl}-betulinic acid. *Retrovirology*, 1:15–25, 2004.

[101] V. Baichwal, H. Austin, B. Brown, R. Mckinnon, K. Yager, V. Kumar, D. Gerrish, M. Anderson, and R. Carlson. Anti-viral Characterization in vitro of a Novel Maturation Inhibitor , MPC-9055. *Montreal, Canada: Program & Abstracts of the 16th Conference on Retroviruses and Opportunistic Infections*, (abstract 561), 2009.

[102] W.S. Blair, J. Cao, L. Jackson, J. Jimenez, Q. Peng, H. Wu, J. Isaacson, S.L. Butler, A. Chu, J. Graham, A.-M. Malfait, M. Tortorella, and A.K. Patick. Identification and characterization of UK-201844, a novel inhibitor that interferes with human immunodeficiency virus type 1 gp160 processing. *Antimicrob Agents Ch*, 51(10): 3554–3561, 2007.

[103] A. Fun, N.M. van Maarseveen, J. Pokorná, R. Maas, P.J. Schipper, J. Konvalinka, and M. Nijhuis. HIV-1 protease inhibitor mutations affect the development of HIV-1 resistance to the maturation inhibitor bevirimat. *Retrovirology*, 8(1):70–82, 2011.

[104] J. Weber, J. Mesters, M. Lepšík, J. Prejdova, M. Švec, J. Šponarová, and J. Konvalinka. Unusual Binding Mode of an HIV-1 Protease Inhibitor Explains its Potency against Multi-drug-resistant Virus Strains. *J Mol Biol*, 324(4):739–754, 2002.

[105] M.E. Quiñones Mateu, J. Weber, H.R. Rangel, and B. Chakraborty. HIV-1 Fitness and Antiretroviral Drug Resistance. *AIDS Rev*, (3):223–242, 2001.

[106] D.D. Richman. Update of the Drug Resistance Mutations in HIV-1 : March 2013. *Topics in Antiviral Medicine*, 21(1):4–12, 2013.

[107] K. Grantz Šašková. *HIV-1 Protease : Insights into Drug Resistance Development.* Phd. thesis, Charles University in Prague, 2010.

[108] M.A. Winters and T.C. Merigan. Insertions in the Human Immunodeficiency Virus

Type 1 Protease and Reverse Transcriptase Genes : Clinical Impact and Molecular Mechanisms. *Antimicrob Agents Ch*, 49(7):2575–2582, 2005.

[109] E.-Y. Kim, M.A. Winters, R.M. Kagan, and T.C. Merigan. Functional Correlates of Insertion Mutations in the Protease Gene of Human Immunodeficiency Virus Type 1 Isolates from Patients. *J Virol*, 75(22):11227–11233, 2001.

[110] M. Kožíšek, K. Grantz Šašková, P. Rezáčová, J. Brynda, N.M. van Maarseveen, D. De Jong, C.A. Boucher, R.M. Kagan, M. Nijhuis, and J. Konvalinka. Ninety-nine is not enough: molecular characterization of inhibitor-resistant human immunodeficiency virus type 1 protease mutants with insertions in the flap region. *J Virol*, 82 (12):5869–5878, 2008.

[111] H. Gatanaga, Y. Suzuki, H. Tsang, K. Yoshimura, M.F. Kavlick, K. Nagashima, R.J. Gorelick, S. Mardy, C. Tang, M.F. Summers, and H. Mitsuya. Amino acid substitutions in Gag protein at non-cleavage sites are indispensable for the development of a high multitude of HIV-1 resistance against protease inhibitors. *J Biol Chem*, 277(8):5952–5961, 2002.

[112] L. Myint, M. Matsuda, Z. Matsuda, Y. Yokomaku, T. Chiba, A. Okano, K. Yamada, and W. Sugiura. Gag Non-Cleavage Site Mutations Contribute to Full Recovery of Viral Fitness in Protease Inhibitor-Resistant Human Immunodeficiency Virus Type 1. *Antimicrob Agents Ch*, 48(2):444–452, 2004.

[113] P.R. Harrigan. Human Immunodeficiency Virus Type 1 Protease Cleavage Site Mutations Associated with Protease Inhibitor Cross-Resistance Selected by Indinavir, Ritonavir, and/or Saquinavir. *J Virol*, 75(2):589–594, 2001.

[114] A. Fun, A.M. Wensing, J. Verheyen, and M. Nijhuis. Human Immunodeficiency Virus Gag and protease: partners in resistance. *Retrovirology*, 9(1):63–77, 2012.

[115] H. Gatanaga, Y. Suzuki, H. Tsang, K. Yoshimura, M.F. Kavlick, K. Nagashima, R.J. Gorelick, S. Mardy, C. Tang, M.F. Summers, and H. Mitsuya. Amino acid substitutions in Gag protein at non-cleavage sites are indispensable for the development

of a high multitude of HIV-1 resistance against protease inhibitors. *J Biol Chem*, 277(8):5952–5961, 2002.

[116] C.M. Parry, M. Kolli, R.E. Myers, P.A. Cane, C.A. Schiffer, and D. Pillay. Three residues in HIV-1 matrix contribute to protease inhibitor susceptibility and replication capacity. *Antimicrob Agents Ch*, 55(3):1106–13, 2011.

[117] C.S. Adamson, S.D. Ablan, I. Boeras, R. Goila-Gaur, F. Soheilian, K. Nagashima, F. Li, K. Salzwedel, M. Sakalian, C.T. Wild, and E.O. Freed. In vitro resistance to the human immunodeficiency virus type 1 maturation inhibitor PA-457 (Bevirimat). *J Virol*, 80(22):10957–10971, 2006.

[118] M.M. Bradford. A rapid and sensitive method for the quantitation of microgram quantities of protein utilizing the principle of protein-dye binding. *Anal biochem*, 7 (72):248–254, 1976.

[119] K. Grantz Šašková, M. Kožíšek, P. Rezáčová, T. Yashina, R.M. Kagan, and J. Konvalinka. Molecular Characterization of Clinical Isolates of Human Immunodeficiency Virus Resistant to the Protease Inhibitor Darunavir. *J Virol*, 83(17):8810–8818, 2009. doi: 10.1128/JVI.00451-09.

[120] J. Ermolieff, X. Lin, and J. Tang. Kinetic properties of saquinavir-resistant mutants of human immunodeficiency virus type 1 protease and their implications in drug resistance in vivo. *Biochemistry*, 36(40):12364–12370, 1997.

[121] E.M. Wondrak, J.M. Louis, H. de Rocquigny, J.C. Chermann, and B.P. Roques. The gag precursor contains a specific HIV-1 protease cleavage site between the NC (P7) and P1 proteins. *Febs Lett*, 333(1-2):21–24, 1993.

[122] S. Campbell and A. Rein. In Vitro Assembly Properties of Human Immunodeficiency Virus Type 1 Gag Protein Lacking the p6 Domain. *J Virol*, 73(3):2270–2279, 1999.

[123] A. De Marco, N.E. Davey, P. Ulbrich, J.M. Phillips, V. Lux, J.D. Riches, T. Fuzik, T. Ruml, H.-G. Kraüsslich, V.M. Vogt, and J.A.G. Briggs. Conserved and variable

features of Gag structure and arrangement in immature retrovirus particles. *J Virol*, 84(22):11729–11736, 2010.

[124] L.-A. Carlson and J.H. Hurley. In vitro reconstitution of the ordered assembly of the endosomal sorting complex required for transport at membrane-bound HIV-1 Gag clusters. *P Natl Acad Sci USA*, 109(42):16928–16933, 2012.

Svoluji k zapůjčení této práce pro studijní účely a prosím, aby byla řádně vedena evidence vypůjčovatelů.

Jméno a příjmenní S adresou	Číslo OP	Datum vypůjčení	Poznámka